

1 **Measurement report: Source apportionment of carbonaceous aerosol using**
2 **dual-carbon isotopes (^{13}C and ^{14}C) and levoglucosan in three northern Chinese**
3 **cities during 2018–2019**

4

5 Huiyizhe Zhao ^{a, c, d}, Zhenchuan Niu ^{a, b, c, d, e, *}, Weijian Zhou ^{a, b, c, d, *}, Sen Wang^f, Xue
6 Feng^g, Shugang Wu ^{a, c}, Xuefeng Lu ^{a, c}, Hua Du ^{a, c}

7 ^a *State Key Laboratory of Loess and Quaternary Geology, CAS Center for Excellence*
8 *in Quaternary Science and Global Change, Institute of Earth Environment, Chinese*
9 *Academy of Sciences, Xi'an 710061, China*

10 ^b *Open Studio for Oceanic-Continental Climate and Environment Changes, Pilot*
11 *National Laboratory for Marine Science and Technology (Qingdao), Qingdao 266061,*
12 *China*

13 ^c *Shaanxi Provincial Key Laboratory of Accelerator Mass Spectrometry Technology*
14 *and Application, Joint Xi'an AMS Center between IEECAS and Xi'an Jiaotong*
15 *University, Xi'an 710061, China*

16 ^d *University of Chinese Academy of Sciences, Beijing 100049, China*

17 ^e *Shaanxi Guanzhong Plain Ecological Environment Change and Comprehensive*
18 *Treatment National Observation and Research Station, Xi'an, China*

19 ^f *Shaanxi Key Laboratory of Earth Surface System and Environmental Carrying*
20 *Capacity, College of Urban and Environmental Sciences, Northwest University, Xi'an,*
21 *China*

22 ^g *Xi'an Institute for Innovative Earth Environment Research, Xi'an, China*

23 **Correspondence:** Zhenchuan Niu (niu^zc@ieecas.cn) and Weijian Zhou
24 (weijian@loess.llqg.ac.cn)

25

26 **Abstract**

27 To investigate, the characteristics and changes in the sources of carbonaceous
28 aerosols in northern Chinese cities after the implementation of the Action Plan for Air
29 Pollution Prevention and Control in 2013, we collected PM_{2.5} samples from three
30 representative inland cities, viz. Beijing (BJ), Xi'an (XA), and Linfen (LF) from
31 January 2018 to April 2019. Elemental carbon (EC), organic carbon (OC),
32 levoglucosan, stable carbon isotope, and radiocarbon were measured in PM_{2.5} to
33 quantify the sources of carbonaceous aerosol, combined with Latin hypercube
34 sampling. The best estimate of source apportionment showed that the emissions from
35 liquid fossil fuels contributed 29.3 ± 12.7%, 24.9 ± 18.0%, and 20.9 ± 12.3% of the
36 total carbon (TC) in BJ, XA, and LF, respectively, whereas coal combustion
37 contributed 15.5 ± 8.8%, 20.9 ± 18.0%, and 42.9 ± 19.4%, respectively. Non-fossil
38 sources accounted for 55 ± 11%, 54 ± 10%, and 36 ± 14% of the TC in BJ, XA, and
39 LF, respectively. In XA, 44.8 ± 26.8% of non-fossil sources was attributed to biomass
40 burning. The highest contributors to OC in LF and XA were fossil sources (74.2 ± 9.6%
41 and 43.2 ± 10.8%, respectively), whereas that in BJ was non-fossil sources, (66.8 ±
42 13.9%). The main contributors to EC were fossil sources, accounting for 91.4 ± 7.5%,
43 66.8 ± 23.8%, and 88.4 ± 10.8% in BJ, XA, and LF, respectively. The decline (6–16%)
44 in fossil source contributions in BJ, since the implementation of the Action Plan
45 indicates the effectiveness of air quality management. We suggest that specific
46 measures targeted to coal combustion, biomass burning and vehicle emissions in
47 different cities, should be strengthened in the future.

49 **Keywords:** carbonaceous aerosols; radiocarbon; stable carbon isotope; biomass
50 burning; fossil fuel combustion; source apportionment

删除的内容: To investigate

删除的内容: ,

删除的内容:

删除的内容: , employing

删除的内容:

删除的内容: 33.6

删除的内容: 9

删除的内容: 6.6

删除的内容: 6.4

删除的内容: 24.6

删除的内容: 13.4

删除的内容: 11.2

删除的内容: 9.1

删除的内容: 19.2

删除的内容: 2.3

删除的内容: 39.2

删除的内容: 20.5

删除的内容: 48.34

删除的内容: 32.01

删除的内容: were

删除的内容: 65.4

删除的内容: 14.9

删除的内容: 4.9

删除的内容: 9.5

删除的内容: in BJ

删除的内容: 56.1

删除的内容: 6.7

删除的内容: 92.9

删除的内容: 6.13

删除的内容: 69.9

删除的内容: 0.9

删除的内容: 90.8

删除的内容: 9.9

删除的内容: of the total EC

删除的内容: 17

删除的内容: and XA

删除的内容: each

删除的内容: ies

删除的内容: ,

90 **1 Introduction**

91 Atmospheric aerosols are extremely complex suspension systems. Carbonaceous
92 aerosols are an important component of atmospheric aerosols, accounting for
93 approximately 10–60% of the total mass of global fine particulate matter (Cao et al.,
94 2003, 2007; Feng et al., 2009). Carbonaceous aerosols contain elemental carbon (EC),
95 organic carbon (OC), and inorganic carbon (IC). IC is mainly derived from sand dust,
96 it has a low concentration and simple composition, and it can be removed via acid
97 treatment (Clarke et al., 1992). EC is produced by incomplete combustion and is
98 directly discharged from pollution sources. It can cause global warming by changing
99 the radiative forcing and ice albedo (Jacobson et al., 2001; Kiehl et al., 2007). OC is a
100 complex mixture of primary and secondary pollutants produced by the combustion of
101 domestic biomass and fossil fuels. It is an important contributor to tropospheric ozone,
102 photochemical smog, and rainwater acidification, and it can significantly impact
103 regional and global environments through biogeochemical cycling (Jacobson et al.,
104 2000; Seinfeld et al., 1998). Therefore, identifying and quantifying the source
105 contributions of carbonaceous aerosols can provide a scientific basis for the
106 management of regional air quality.

107 The natural radiocarbon (^{14}C) is completely depleted in fossil emissions, due to
108 the age of fossil fuels well above the half-life of ^{14}C (5730 years), whereas non-fossil
109 sources show the similar ^{14}C as environment (Szidat, 2009; Heal, 2014). Therefore,
110 ^{14}C can be used to study the source of atmospheric particulate matter and to
111 quantitatively and accurately distinguish the contributions of fossil and non-fossil
112 sources (Clayton et al., 1955; Currie, 2000; Szidat, 2009). In recent decades, this
113 method has been widely used to trace non-fossil carbonaceous aerosols in various
114 regions (Ceburnis et al., 2011; Lewis et al., 2004; Szidat et al., 2009; Vonwiller et al.,

115 | 2017; Yang et al., 2005; Zhang et al., 2012, 2017a). Stable carbon isotope (^{13}C) is a
116 | useful geochemical marker that can provide valuable information about both the
117 | sources and atmospheric processing of carbonaceous aerosols (López-Veneroni, 2009;
118 | Widory, 2006), and it has been applied in various types of environmental research to
119 | identify emission sources (Cachier et al., 1985, 1986; Cao et al., 2011; Chesselet et al.,
120 | 1981; Fang et al., 2017; Kawashima & Haneishi, 2012; Kirillova et al., 2013). The
121 | analysis of $^{13}\text{C}/^{12}\text{C}$ can refine ^{14}C source apportionment because both coal and liquid
122 | fossil fuels are depleted of ^{14}C while their ^{13}C source signatures are different
123 | (Andersson et al., 2015; Li et al., 2016; Winiger et al., 2017). Levoglucosan (Lev), a
124 | thermal degradation product of cellulose combustion, is a common molecular tracer
125 | that can be used to evaluate the contribution of biomass burning (Hoffmann et al.,
126 | 2010; Locker et al., 1988; Simoneit et al., 1999). The combination of the carbon
127 | isotope analysis and Lev can further divide the contributions of different
128 | carbonaceous sources. Some studies have confirmed the feasibility of this
129 | combination (Claeys et al., 2010; Gelencsér et al., 2007; Genberg et al., 2011; Huang
130 | et al., 2014; Kumagai et al., 2010; Liu et al., 2013; Niu et al., 2013; Zhang et al.,
131 | 2015).

删除的内容: they have

132 | Cities in northern China have been affected by severe haze for several decades
133 | (Cao et al., 2012; Han et al., 2016; Sun et al., 2006; Wang et al., 1990). After the
134 | Action Plan for Air Pollution Prevention and Control (hereafter simplified as “Action
135 | Plan”) was promulgated in 2013, all parts of China responded to the issue and held
136 | numerous air quality management practices (CSC, 2013). In 2020, the average $\text{PM}_{2.5}$
137 | concentration in Chinese cities across the country decreased by 54.2% compared to
138 | that in 2013 (MEE, 2014, 2021). In 2020, the proportion of clean energy consumption,
139 | such as that of natural gas and electricity, increased by 7.9% compared to that in 2013,

141 and the proportion of coal combustion decreased by 9.7% (NBS, 2021). Before the
142 Action Plan, fossil fuel sources were identified as the main contributor to
143 carbonaceous aerosols in Chinese cities (56–81%) (Ni et al., 2018, Niu et al., 2013,
144 Shao et al., 1996; Sun et al., 2012; Yang et al., 2005). In this study, we aimed to
145 determine the main contribution of the current carbonaceous aerosols in northern
146 Chinese cities. Also, we aimed to identify whether changes in energy type and
147 emission control caused a change in the source of carbonaceous aerosols.

148 To address those issues, we conducted a source apportionment of carbonaceous
149 aerosols based on yearly measurements of OC, EC, Lev, ^{13}C , and ^{14}C in $\text{PM}_{2.5}$,
150 combined with Latin hypercube sampling (LHS), in three representative northern
151 Chinese cities during 2018–2019. This study provides a comprehensive understanding
152 of current sources of carbonaceous aerosol after the implementation of the Action
153 Plan in Chinese cities.

154

155 **2 Methods**

156 **2.1 Research sites**

157 We selected one urban sampling site in Beijing (BJ), one in Xi'an (XA), and one
158 in Linfen (LF) (Fig. 1). BJ is the capital of China, one of the largest megacities in the
159 world, and the central city of the Beijing–Tianjin–Hebei economic region. It has a
160 population of more than 20 million and has experienced serious air pollution problems
161 in the past few decades. XA, the capital of Shaanxi Province, is the ninth-largest
162 central city and an important city of the Northwest Economic Belt in China. It is
163 located in a basin surrounded by mountains on three sides, where atmospheric
164 pollutants are discharged mainly from the basin and are less affected by other urban
165 areas (Cao et al., 2009; Shen et al., 2011). LF is located in western Shanxi Province

166 and is one of the representative cities in the northern air-polluted region. Shanxi
167 Province is the center of Chinese energy production and chemical metallurgy
168 industries; its coal production and consumption were approximately 736.81 million
169 tons and 349.07 million tons, accounting for 27.1% and 12.4% of the Chinese total in
170 2019, respectively (NBS, 2020; SPBS, 2020). The air quality in LF was ranked in the
171 worst ten in China from 2018 to 2020 (MEE, 2019, 2020, 2021). According to the
172 pollutant data released by the National Air Quality Real-time Release Platform,
173 Ministry of Ecology and Environment (MEE) of the People's Republic of China
174 (<http://106.37.208.233:20035/>), the daily average atmospheric SO₂ concentration in
175 LF exceeded 850 μg m⁻³ on January 4th, 2017, XA and LF heavily suffer from air
176 pollution in the Fenwei Plain. In July 2018, the State Council issued the Three-Year
177 Action Plan to Win the Blue Sky Defense War. This included the Fenwei Plain as one
178 of the key areas in which to prevent and control pollution (CSC, 2018).

删除的内容: 05

删除的内容: 2

删除的内容: China Central Television (CCTV) reports,

删除的内容:

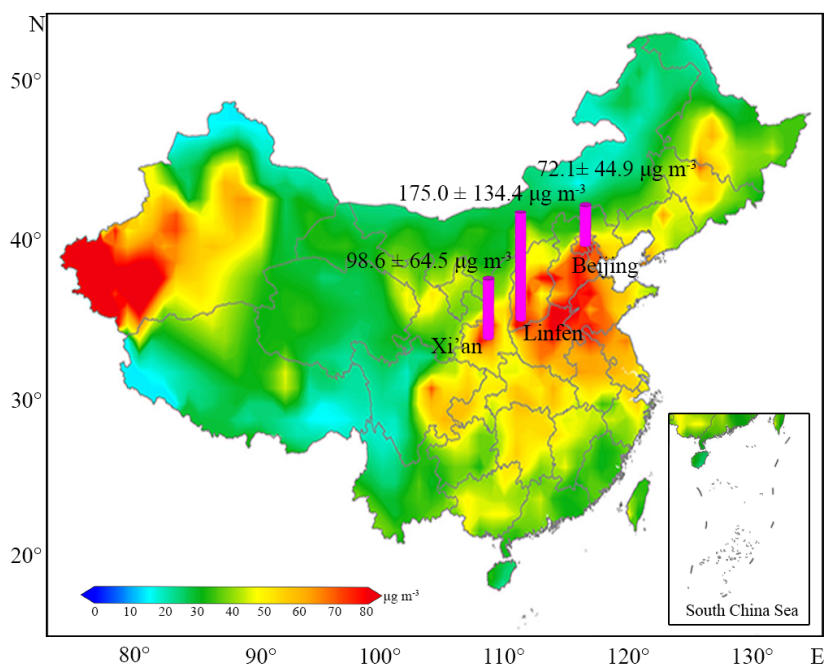
删除的内容: 1000

删除的内容: several times during

删除的内容: (CCTV, 2017)

删除的内容: this

179 The first site was located in the northwest of BJ, on the rooftop of the Research
180 Center for Eco-Environmental Sciences, Chinese Academy of Sciences (40°0'33" N,
181 116°20'38" E). The site was approximately 200 m from the road. The second site was
182 located southwest of XA, on the rooftop of the School of Urban and Environmental
183 Sciences in Northwest University (34°15'36" N, 108°88'53" E). Living quarters and
184 teaching areas were located around these two sampling sites. The third site was
185 located in Houma, a county-level city of LF, on the rooftop of a residential building
186 (35°63'56" N, 111°39'53" E). There was no industrial pollution near each site and
187 they were representative urban sites.



197

198 Fig. 1 Locations and PM_{2.5} concentration of Beijing (BJ), Xi'an (XA), and Linfen
 199 (LF). The background map shows the distribution of PM_{2.5} concentrations in most of
 200 China from 2015 to 2019 (Li et al., 2021a). The pink bars are the average PM_{2.5}
 201 concentrations of the samples collected in this study during 2018 to 2019.

202

203 2.2 Sample collection

204 At BJ and XA, PM_{2.5}, samples were collected on the 7th, 14th, 21st, and 28th of
 205 each month from April 28, 2018, to April 21, 2019. In LF, seven consecutive days in
 206 each season were selected for sample collection, and the sampling periods were
 207 concentrated in January, April, July, and October 2018. A total of 124 24-hour (10
 208 a.m. to 10 a.m. on the following day) PM_{2.5} samples and 4 field blanks were obtained.

209 Samples in each city were collected continuously on pre-baked quartz fiber
 210 filters (203 mm × 254 mm, Whatman UK) using a high-volume (1.05 m³ min⁻¹)

211 | sampler (TH-1000CII). The sampler was equipped with an impact collector to collect
212 | the particles less than 2.5 μm in aerodynamic diameter. To remove the existing carbon
213 | in the materials, the filter and foil used for wrapping should be baked in a muffle
214 | furnace at 375 $^{\circ}\text{C}$ for 5 h before use. After sampling, the filters were folded, wrapped
215 | in pre-baked aluminum foil, and stored at -18°C . All filters were weighed after
216 | equilibrating at $25 \pm 1^{\circ}\text{C}$ and $52 \pm 5\%$ humidity for more than 24 h. The $\text{PM}_{2.5}$ mass
217 | loadings were determined gravimetrically using a 0.1 mg sensitivity electronic
218 | microbalance. Carbonate has been removed from the filters by spraying with
219 | hydrochloric acid (1 mol L^{-1}) before measurement.

删除的内容: until analysis

220 | **2.3 OC and EC analyses**

221 | Filter pieces of 0.526 cm^2 were used to measure the OC and EC using a DRI
222 | Model 2001 (Thermal/Optical Carbon Analyzer) at the Institute of Earth Environment,
223 | Chinese Academy of Sciences. The Interagency Monitoring of Protected Visual
224 | Environments (IMPROVE) thermal/optical reflectance protocol must be followed
225 | because OC and EC have different oxidation priorities under different temperatures
226 | (Cao et al., 2007; Chow & Watson, 2002). OC and EC were defined as $\text{OC1} + \text{OC2} +$
227 | $\text{OC3} + \text{OC4} + \text{OP}$ and $\text{EC1} + \text{EC2} + \text{EC3} - \text{OP}$, respectively, in accordance with the
228 | IMPROVE protocol (Chow et al., 2004). Sample analysis results were corrected by
229 | the average blank and standard sucrose concentrations of OC and EC, respectively.

230 | **2.4 Lev analysis**

231 | The molecular tracer (Lev) was determined by high-performance anion exchange
232 | chromatography with pulsed amperometric detection (HPAEC-PAD) method at the
233 | South China Institute of Environmental Science, Ministry of Ecology and
234 | Environment. A quartz filter sample (2 cm^2) was extracted with 3 ml of deionized
235 | water in a prebaked glass bottle under ultrasonic agitation and was subsequently

237 analyzed using a Dionex ICS-3000 system after filtration. The separation requires an
238 equilibrium period, isocratic elution, and gradient elution. (For a specific description,
239 refer to Zhang et al., 2013.) The instrument sample loop was 100 μL and the detection
240 limit of Lev was $1 \times 10^{-8} \mu\text{g ml}^{-1}$.

241 Recent studies indicated that Lev was degraded to some extent during
242 atmospheric transportation, and about 25% of them came from other non-biomass
243 burning sources (Hoffmann et al., 2010; Wu et al., 2021). Therefore, correction of the
244 biomass burning source lev (Lev_{bb}) is required before the source apportionment:

$$245 \quad \text{Lev}_{\text{bb}} = \frac{\text{Lev} \times 0.75}{p} \quad (1)$$

246 where p (0.4–0.65) is the degradation rate of Lev, which has different
247 characteristics in each seasons. For specific p value in each season, please refer to the
248 research of Li et al. (2021b).

249 2.5 Stable carbon **isotope** analysis

250 The ^{13}C compositions were determined using a gas isotopic analyzer (Picarro
251 G2131-i) in conjunction with an elemental analyzer (Elemental Combustion System
252 4010) at the Institute of Earth Environment, Chinese Academy of Sciences.
253 Specifically, 0.2–0.4 mgC of sample has been placed in a precombusted tin capsule
254 (6 \times 10 mm) and the air was removed by squeezing. The samples were tested at 980 $^{\circ}\text{C}$
255 and 650 $^{\circ}\text{C}$ with 70–80 ml min^{-1} helium as the carrier gas and 20–30 ml min^{-1} oxygen
256 as the reaction gas. The resulting gas mixture was then collected in Gas Isotopic
257 Analyzer (Bachar et al., 2020). Urea standard (CAS Number: 57-13-6) was used as
258 standard sample. ^{13}C data are expressed in delta notation with respect to Vienna Pee
259 Dee Belemnite (VPDB) (Coplen, 1996):

$$260 \quad \delta^{13}\text{C} = \left[\frac{^{13}\text{C}/^{12}\text{C}_{\text{Sample}}}{^{13}\text{C}/^{12}\text{C}_{\text{VPDB}}} - 1 \right] \times 1000\text{‰}$$

删除的内容: was

删除的内容: 1

263 **2.6 Radiocarbon analysis**

264 The ¹⁴C samples were prepared and tested in the laboratory of Xi'an accelerator
265 mass spectrometer (AMS) Center. The processed sample was packed in a sealed
266 quartz tube with a silver wire and excessive CuO. The solid sample was then
267 combusted at 850 °C for 2.5 h to convert it into gas after the vacuum degree was less
268 than 5×10⁻⁵ mbar. The gas sample was passed through a liquid nitrogen cold trap
269 (-196 °C) to freeze CO₂ and water vapor, and then passed through an ethanol-liquid
270 nitrogen cold trap (-90 °C) to remove water vapor and purify CO₂ (Turnbull et al.,
271 2007; Zhou et al., 2014). The collected CO₂ was reduced to graphite via a reduction
272 reaction with zinc particles and iron powder as the reductant and catalyst, respectively
273 (Jull, 2007; Slota et al., 1987). The graphite was pressed into an aluminum holder and
274 measured using a 3 Megavolt AMS, with a precision of 3‰ (Zhou et al., 2006, 2007).
275 Forty-nine targets were arranged in sequence in the sample fixed wheel, including
276 forty samples, six OX-II standard samples, two anthracite standard samples and one
277 sugar carbon standard sample each time. AMS online δ¹³C of was used for isotope
278 fractionation correction.

279 The ¹⁴C results were expressed as a fraction of modern carbon (f_M) (Currie, 2000;
280 Mook & Plicht, 1999). It defines as the ¹⁴C/¹²C ratio of the sample related to the
281 isotopic ratio of the reference year 1950 (Stuiver & Polach, 1977):

282 $f_M = (^{14}\text{C}/^{12}\text{C}_{\text{Sample}})/(^{14}\text{C}/^{12}\text{C}_{1950})$.

283 Atmospheric nuclear bomb tests in the late 1950s and the early 1960s released a
284 large amount of ¹⁴C, and the ratio of ¹⁴C/¹²C in atmospheric CO₂ roughly doubled in
285 the mid-1960s (Hua & Barbetti, 2004; Levin et al., 2003, 2010; Lewis et al., 2004;
286 Niu et al., 2021). However, f_M in the atmosphere has been decreasing because of the
287 dilution effect produced by the absorption of marine and terrestrial biospheres and the

删除的内容: c

删除的内容: ontainer

删除的内容: MV

删除的内容: 2

292 release of fossil fuels. In recent years, studies on background ^{14}C in China and
 293 other countries have shown that the f_M value in the atmosphere has decreased and
 294 approached 1 (Hammer et al., 2017; Niu et al., 2016). This means that the impact of
 295 the nuclear explosions has almost disappeared for current atmosphere, and the change
 296 in current atmospheric ^{14}C was mainly influenced by the regional natural carbon cycle
 297 and fossil fuel CO_2 emissions. Thus, the f_M values were not corrected in this study,
 298 because the material used for biomass burning in China was mainly from crop straw
 299 (Fu et al., 2012; Street et al., 2003b; Yan et al., 2006; Zhang et al., 2017b), and the
 300 influence of atmospheric nuclear bomb test has basically vanished for the annual
 301 plants.

302 Non-fossil fractions (f_{nf}) and fossil fractions (f_{f}) were determined from the f_M
 303 values.

304 $f_{\text{nf}} = f_M \times 100\%$ (4)

305 $f_{\text{f}} = (1 - f_M) \times 100\%$ (5)

306 **2.7 Source apportionment of total carbon using ^{14}C and ^{13}C**

307 To study the contribution of each fossil source to the total carbon (TC), we used
 308 the principle of isotopic chemical mass balance to further separate fossil sources into
 309 liquid fossil fuels and coal. Since the amount of carbonaceous aerosol produced by
 310 natural gas is very low compared to coal and liquid fossil combustion, its contribution
 311 was not considered here (Chen et al., 2005; England et al., 2002; Guo et al., 2014; Yan
 312 et al., 2010). In this part, ^{13}C and ^{14}C were combined to calculate the contributions of
 313 non-fossil, coal, and liquid fossil sources.

314 $f_{\text{nf}} \times \delta^{13}\text{C}_{\text{nf}} + f_{\text{coal}} \times \delta^{13}\text{C}_{\text{coal}} + f_{\text{liq.fossil}} \times \delta^{13}\text{C}_{\text{liq.fossil}} = \delta^{13}\text{C}_{\text{sample}} + \beta$ (6)

315 $f_{\text{coal}} + f_{\text{liq.fossil}} = f_{\text{f}}$ (7)

316 where, f_{nf} , f_{coal} , and $f_{\text{liq.fossil}}$ represent the proportions of non-fossil source, coal and

删除的内容: 3

删除的内容: 4

删除的内容: 5

删除的内容: 6

删除的内容: $\delta^{13}\text{C}_{\text{sample}}$ is the $\delta^{13}\text{C}$ of the samples at each site;

323 liquid fossil combustion, respectively, $\delta^{13}\text{C}_{\text{nf}}$, $\delta^{13}\text{C}_{\text{coal}}$, and $\delta^{13}\text{C}_{\text{liq.fossil}}$ represent $\delta^{13}\text{C}$
324 from the corresponding sources. $\delta^{13}\text{C}_{\text{sample}}$ is the $\delta^{13}\text{C}$ of the samples at each site, and
325 β is a small correction.

删除的内容: each source; and

326 Since the formation process of OC can cause the fractionation of ^{13}C , with a
327 range mainly in 0.03–1.40 ‰ (mean 0.2‰) (Aggarwal and Kawamura, 2008; Cao et
328 al, 2011; Ho et al., 2006; Zhao et al., 2018), a small correction (0.2‰) was made for
329 the $\delta^{13}\text{C}$ sample used in Eq. 6. The selection of the reference value was described in
330 detail in Section 2.9.

删除的内容: is

331 **2.8 Source apportionment of OC and EC using ^{14}C and Lev_{bb}**

332 The method combines ^{14}C with the concentration of carbon components and a
333 molecular tracer (Lev_{bb}) to quantify the sources of OC and EC. Carbon was assumed
334 to originate from fossil fuel combustion, biomass burning, and other non-fossil
335 emissions (Gelencsér et al., 2007). The following is a simple calculation method.

336 EC consists of biomass burning (EC_{bb}) and fossil fuel combustion (EC_{ff}).

$$337 \text{EC} = \text{EC}_{\text{ff}} + \text{EC}_{\text{bb}}$$

(8)

删除的内容: 7

338 EC_{bb} was calculated based on the Lev_{bb} concentration and the estimated
339 $\text{EC}_{\text{bb}}/\text{Lev}_{\text{bb}}$ ratio:

$$340 \text{EC}_{\text{bb}} = \text{Lev}_{\text{bb}} \times (\text{EC}_{\text{bb}}/\text{Lev}_{\text{bb}}) = \text{Lev}_{\text{bb}} \times [(\text{EC}/\text{OC})_{\text{bb}}/(\text{Lev}_{\text{bb}}/\text{OC}_{\text{bb}})]$$

(9)

删除的内容: 8

341 Then, EC_{ff} was calculated by subtraction (Eq. 8).

删除的内容: 7

342 OC consists of OC from biomass burning (OC_{bb}), fossil fuel combustion (OC_{ff}),
343 and other sources (OC_{other}), including primary and secondary biogenic OC and SOC
344 (secondary organic carbon) from non-fossil emissions.

$$345 \text{OC} = \text{OC}_{\text{bb}} + \text{OC}_{\text{ff}} + \text{OC}_{\text{other}}$$

(10)

删除的内容: 9

346 OC_{bb} was calculated based on the Lev_{bb} concentration and the estimated
347 $\text{Lev}_{\text{bb}}/\text{OC}_{\text{bb}}$ ratio:

354 $OC_{bb} = Lev_{bb}/(Lev_{bb}/OC_{bb})$ (11)

删除的内容: 10

355 OC_{other} was calculated by balancing the ^{14}C content that was not attributed to
356 OC_{bb} .

357 $OC_{other} = (OC \times f_{nf}(OC) - OC_{bb} \times f_M(bb))/f_M(nf)$ (12)

删除的内容: 11

358 Furthermore, $f_{nf}(OC)$ was calculated based on the ^{14}C concentration measured in
359 the sample (detailed description of the formulas can be found in Genberg et al., 2011);
360 $f_M(bb)$ and $f_M(nf)$ are the ^{14}C concentrations in biomass burning and other non-fossil
361 emissions, respectively.

362 Finally, OC_{ff} was calculated by subtraction (Eq. 10).

删除的内容: 9

363 2.9 Uncertainties of source apportionment

364 Some uncertainties exist in some parameters in Eqs. 5–11 and need to be
365 evaluated. Table 1 lists the range of reference values used in this study. The ratios

366 Lev_{bb}/OC_{bb} and EC_{bb}/OC_{bb} depend on the type of biofuel and the burning conditions
367 (Oros et al., 2001a, b). In foreign studies, the most common distributions of

368 Lev_{bb}/OC_{bb} and EC_{bb}/OC_{bb} are 0.08–0.2 and 0.07–0.45, respectively (Gelencsér et al.,
369 2007; Puxbaum et al., 2007; Szidat et al., 2006). The distribution ranges of

370 Lev_{bb}/OC_{bb} and EC_{bb}/OC_{bb} burned by trees, shrubs, and rice are approximately
371 0.01–0.04 and 0.05–0.31, respectively (Engling et al., 2006, 2009; Wang et al., 2009).

372 Zhang et al. (2007) found that the values of Lev_{bb}/OC_{bb} and EC_{bb}/OC_{bb} in the cereal
373 straw of BJ were 0.08 and 0.13, respectively.

374 The $\delta^{13}C$ of aerosols derived from liquid fossil fuels (gasoline and diesel oil) was
375 approximately ~~-31~~‰ to -25 ‰ (Agnihotri et al., 2011; Huang et al., 2006;

删除的内容: 28

376 Lopez-Veneroni, 2009; [Pugliese et al., 2017](#); [Vardag et al., 2015](#); Widory, 2006). The
377 $\delta^{13}C$ derived from coal combustion was relatively high, ranging from -25 ‰ to -21 ‰

378 (Agnihotri et al., 2011; [Pugliese et al., 2017](#); Widory, 2006). The results of Agnihotri

383 et al. (2011) showed that the $\delta^{13}\text{C}$ characteristic of biomass burning emissions ranged
 384 from -25.9‰ to -29.4‰ . Smith & Epstein (1971) found that plants with C3 (e.g.,
 385 wheat, soybeans, and most woody plants) and C4 (e.g., corn, grass, and sugar cane)
 386 metabolism had significantly different $\delta^{13}\text{C}$, with an average of -27‰ and -13‰ ,
 387 respectively. In other studies, these two types of plant-derived aerosols had different
 388 characteristics; the ^{13}C from C3 and C4 plants ranged from approximately -23.9‰ to
 389 -32‰ (Moura et al., 2008; Turekian et al., 1998) and from -11.5‰ to -13.5‰
 390 (Martinelli et al., 2002), respectively.

Table 1. Values with limits of input parameters for source apportionment using Latin hypercube sampling (LHS).

Parameters	Low	Probable value	High
Lev _{bb} /OC _{bb}	0.01	0.11	0.20
EC _{bb} /OC _{bb}	0.13	0.22	0.31
$\delta^{13}\text{C}_{\text{liq.fossil}} (\text{‰})$	-31.00	-27.00	-25.00
$\delta^{13}\text{C}_{\text{Coal}} (\text{‰})$	-25.00	-22.95	-21.00
$\delta^{13}\text{C}_{\text{nf}}^{\text{a}} (\text{‰})$	-26.00	-25.25	-24.00
$\delta^{13}\text{C}_{\text{nf}}^{\text{b}} (\text{‰})$	-27.00	-26.50	-25.00

Agnihotri et al., 2011; Engling et al., 2006, 2009; Gelencsér et al., 2007; Huang et al., 2006; Lopez-Veneroni, 2009; Martinelli et al., 2002; Moura et al., 2008; Oros et al., 2001a, b; Puxbaum et al., 2007; Smith & Epstein, 1971; Szidat et al., 2006; Turekian et al., 1998; Wang et al., 2009; Widory, 2006; Zhang et al., 2007.

^a Values used in BJ/LF

^b Values used in XA

391 Because of the differences in the structure of biomass fuels in different cities, we
 392 selected the $\delta^{13}\text{C}$ value based on the current status of biomass fuel used in research

397 regions. In China, biomass fuels mainly include crop residues, branches, and leaves,
398 and the amount of perennial wood is quite small (Zhang et al., 2015). BJ has a small
399 area of arable land, with low agricultural output and corn production (BJMBS, 2020).
400 The neighboring province, Hebei, is a large agricultural province that produces a large
401 amount of wheat and corn annually; the latter has a larger sown area (PGHP, 2020).
402 Shanxi Province also mainly produces wheat and corn; however, the sown area of
403 corn is more than three times that of wheat (SPBS, 2020). Agricultural production in
404 XA and the surrounding Guanzhong area is relatively large. The agricultural structure
405 is dominated by wheat and corn, and their sown areas are not very different (SAPBS,
406 2020). This shows that the $\delta^{13}\text{C}$ of agricultural straw burning in LF is likely to be
407 higher and that in XA may be lower. Some studies considered that $\delta^{13}\text{C}$ used for
408 quantitative mass-balance source apportionment calculations from biomass burning
409 should mainly be defined as C3 plants (Anderson et al., 2015; Fang et al., 2017; Ni et
410 al., 2020). Based on this information, the $\delta^{13}\text{C}$ value of biomass burning in BJ and LF
411 was found to be approximately -26‰ to -24‰ , and that in XA is likely to be from
412 approximately -27‰ to -25‰ . According to the researches about biomass burning
413 type, perennial biomass fuel was less frequently used in China (Fu et al., 2012; Street
414 et al., 2003b; Yan et al., 2006; Zhang et al., 2017b), the impact of nuclear explosions
415 on ^{14}C data can be ignored, and the $f_M(\text{nf})$ and $f_M(\text{bb})$ of the local station should be
416 close to the atmospheric value.

417 To evaluate the uncertainties of the quantification of source contributions, which
418 resulted from the uncertainties of the parameters used, we used Python software to
419 generate 3000 random variable simulations based on the LHS method (Gelencsér et
420 al., 2007). After excluding part of the out-of-range data, the median value of the
421 remaining simulations of each sample were considered as the best estimate. The

删除的内容: Nuclear bomb tests in the late 1950s and the early 1960s released a large amount of ^{14}C , and the ratio of $^{14}\text{C}/^{12}\text{C}$ in atmospheric CO_2 roughly doubled in the mid-1960s (Hua & Barbetti, 2004; Levin et al., 2003, 2010; Lewis et al., 2004; Niu et al., 2021). However, f_M in the atmosphere has been decreasing because of the dilution effect produced by the absorption of marine and terrestrial biospheres and the release of fossil fuels. In recent years, studies on background $^{14}\text{CO}_2$ in China and other countries have shown that the f_M value in the atmosphere has decreased and approached 1 (Hammer et al., 2017; Niu et al., 2016). This means that the impact of the nuclear explosions has almost disappeared, and the current changes in atmospheric ^{14}C was mainly influenced by the regional natural carbon cycle and fossil fuel CO_2 emissions. As

已移动 [1]: emissions.

删除的内容: is

448 results of the uncertainties analysis had been discussed further in Section 3.6.

449 2.10 Air mass backward trajectory analysis

450 For Backward trajectory analysis, air-mass back trajectories from the previous 48
451 h were determined by using the HYbrid Single-Particle Lagrangian Integrated
452 Trajectory (HYSPLIT) model (Draxler and Hess, 1998) at three different endpoint
453 heights (e.g., 100 m, 500 m, and 1000 m) and a time interval of 6 h for sampling day
454 (<https://www.arl.noaa.gov/>).

455

456 3 Results and discussion

457 3.1 Characteristics and variation of carbonaceous components

458 During the sampling period, the average mass concentration of PM_{2.5} in BJ, XA,
459 and LF was 72.1 ± 44.9 , 98.6 ± 64.5 , and 175.0 ± 134.4 $\mu\text{g m}^{-3}$, respectively. All
460 concentrations were higher in winter and lower in summer; LF showed the highest
461 value of 368.7 ± 75.0 $\mu\text{g m}^{-3}$ in winter.

462 Fig. 2 shows the changes in OC and EC and their ratios at the sampling sites. The
463 carbon components in the BJ, XA, and LF samples accounted for approximately 17.5
464 $\pm 6.0\%$, $21.5 \pm 21.0\%$, and $17.8 \pm 7.2\%$ of PM_{2.5}, respectively. Both OC and EC were
465 changing simultaneously and were characterized by low carbonaceous concentrations
466 in summer (OC: 8.9 ± 3.7 $\mu\text{g m}^{-3}$; EC: 1.6 ± 0.9 $\mu\text{g m}^{-3}$) and high concentrations in
467 winter (OC: 69.2 ± 58.9 $\mu\text{g m}^{-3}$; EC: 11.8 ± 7.9 $\mu\text{g m}^{-3}$). The average OC/EC ratios in
468 BJ, XA, and LF were 4.0 ± 1.4 , 9.0 ± 6.1 , and 6.6 ± 2.0 , respectively. Recent studies
469 have shown that the average ratio of OC/EC in BJ, XA, and Shanxi Province was
470 approximately 1.22–6.5 (Han et al., 2016; Ji et al., 2018; Wang et al., 2015; Zhao et
471 al., 2013). Generally, secondary OC (SOC) is considered to occur when OC/EC > 2
472 (Castro et al., 1999; Novakov et al., 2005; Turpin & Huntzicker, 1995). Additionally,

删除的内容: 07

删除的内容: 87

删除的内容: 1

删除的内容: 3

删除的内容: 0

删除的内容: 1

删除的内容: 1

删除的内容: 74

删除的内容: 96

删除的内容: 85

删除的内容: 1

删除的内容: 56

删除的内容: 2

删除的内容: 2

删除的内容: 4

删除的内容: 1

删除的内容: 88

删除的内容: 3.95

删除的内容: 1

删除的内容: 8.98

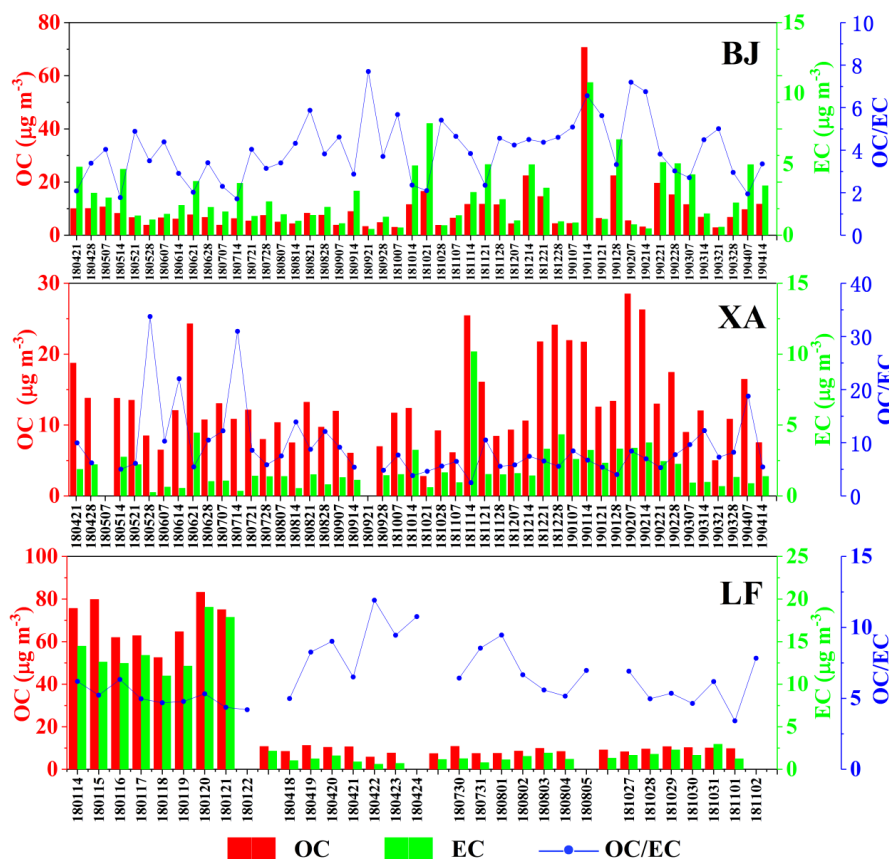
删除的内容: 09

删除的内容: 58

删除的内容: 4

496 [the use of biomass fuels can also enhance the OC/EC ratio \(Popovicheva et al., 2014;](#)
 497 [Rajput et al., 2011\)](#). Therefore, [the high OC/EC ratio indicates that carbonaceous](#)
 498 [aerosols contained a large number of SOCs or biomass burning sources](#), especially in
 499 XA.

删除的内容: The
 删除的内容: all



500
 501 Fig. 2 Variations of elemental carbon (EC), organic carbon (OC) and their ratios in
 502 PM_{2.5} at the sampling sites in Beijing (BJ), Xi'an (XA), and Linfen (LF) (date,
 503 "yymmdd").

504 The average mass concentrations of TC, OC, and EC at the sampling site in BJ
 505 were 12.5 ± 11.8 , 9.7 ± 10.0 , and 2.8 ± 2.1 $\mu\text{gC m}^{-3}$. The concentration of carbon
 506 components was relatively stable in spring and summer but fluctuated greatly in
 507 autumn and winter. The concentration of carbon components in most cases was close

删除的内容: 0
 删除的内容: 79
 删除的内容: 3
 删除的内容: 9.99
 删除的内容: 77
 删除的内容: 2

516 to that of other periods, but there was a rapid increase in autumn and winter. The
517 highest TC value was observed in the middle of January 2019 ($81.5 \mu\text{gC m}^{-3}$).

518 The average concentrations of TC, OC, and EC in XA were 14.6 ± 7.5 , $12.8 \pm$
519 6.3 , and $1.9 \pm 1.6 \mu\text{gC m}^{-3}$, respectively. In contrast to that in BJ, the concentration of
520 the carbon components in XA fluctuated greatly throughout the year. Specifically, the
521 concentration was lower from July to October and significantly higher from
522 December to February. However, there were high concentrations of TC on some days
523 in spring and summer, such as June 21, 2018, with the concentration reaching 28.8
524 $\mu\text{gC m}^{-3}$.

525 The average concentrations of TC, OC, and EC in LF were 35.7 ± 36.5 , $30.0 \pm$
526 30.4 , and $5.6 \pm 6.2 \mu\text{gC m}^{-3}$, respectively. In contrast to those in BJ and XA, the
527 concentration of the carbon components in LF was persistently high in winter and
528 stable and low in other seasons.

529

530 3.2 Variations of ^{14}C

531 The ^{14}C results showed that the average f_{nf} values in BJ, XA, and LF were $54 \pm$
532 11% , $54 \pm 10\%$, and $36 \pm 14\%$, respectively. Non-fossil sources were the main
533 contributors in the BJ and XA samples (Fig. 3). Furthermore, the f_{nf} in the BJ samples
534 showed a higher average value in spring ($59 \pm 6\%$), whereas that in the XA samples
535 had higher average values in autumn (f_{nf} , $59 \pm 7\%$) and winter (f_{nf} , $63 \pm 6\%$). In the
536 LF samples, fossil sources were the main contributors, contributing $81 \pm 1\%$ in
537 winter.

538 By analyzing the f_{nf} characteristics of samples with different pollution levels
539 based on the $\text{PM}_{2.5}$ concentration, we can study the causes and characteristics of air
540 pollution more effectively. Using the relevant classification index of the daily average

删除的内容: 1

删除的内容: Fig. 2 Variations of carbon components and their ratios in $\text{PM}_{2.5}$ at the sampling sites in Beijing (BJ), Xi'an (XA), and Linfen (LF) (date, "yymmdd"). .

删除的内容: 4

删除的内容: 2

删除的内容: 76

删除的内容: 26

删除的内容: 89

删除的内容: 1

删除的内容: 75

删除的内容: 66

删除的内容: 3

删除的内容: 3

删除的内容: 0

删除的内容: 4

删除的内容: 4

删除的内容: 55

删除的内容: 64

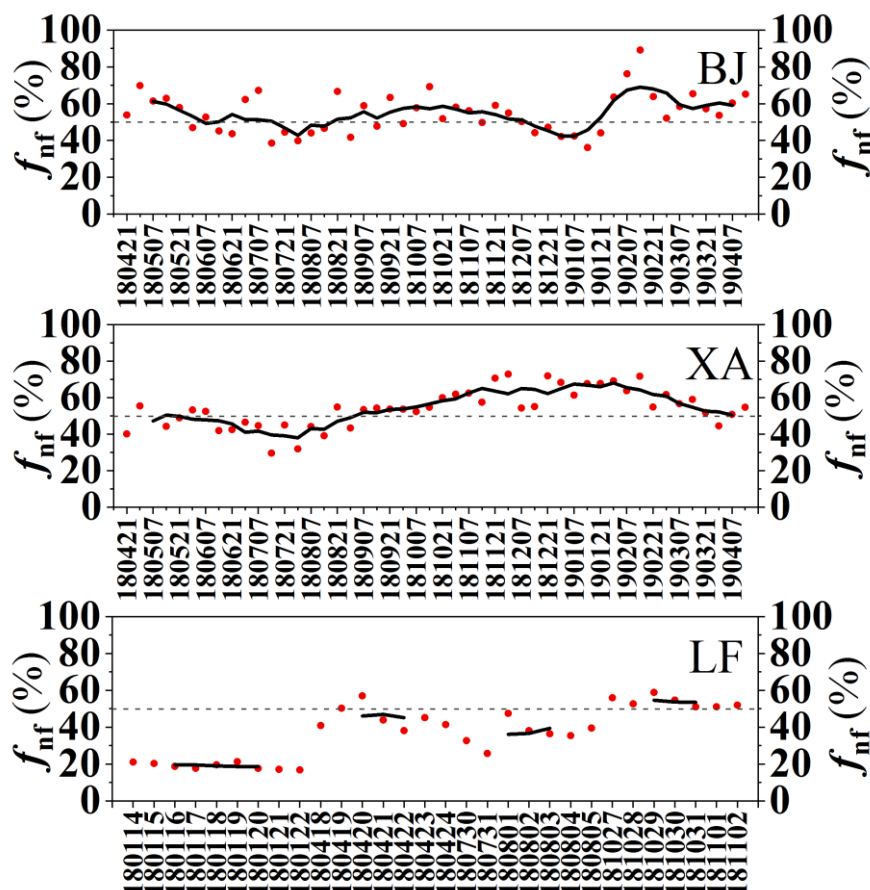
删除的内容: 80

563 PM_{2.5} concentration in the Technical Regulation on Ambient Air Quality Index (MEE,
564 2012), we divided the samples into clean (with a concentration of less than 75 $\mu\text{g m}^{-3}$),
565 regular (with a concentration between 75 and 150 $\mu\text{g m}^{-3}$), and polluted (with a
566 concentration greater than 150 $\mu\text{g m}^{-3}$). The f_{nf} value in most samples in BJ ($44 \pm 8\%$)
567 and LF ($19 \pm 2\%$) was lower during serious air pollution (Fig. 4), indicating that the
568 high concentrations of aerosols in BJ and LF were more affected by fossil sources.
569 One BJ sample had a low f_{nf} value (36%) in January and another had a high f_{nf} value
570 (89%) in February. These samples were collected when the atmosphere was severely
571 polluted and very clean, respectively. This might indicate that emissions from fossil
572 fuel sources are a decisive factor of air pollution in BJ. In the XA samples, when the
573 atmosphere was clean, f_{nf} decreased by 2–3%, indicating that the carbonaceous
574 aerosol pollution may be more affected by biomass burning or secondary non-fossil
575 sources from local emissions.

576 As can be seen in Fig. 5, the contribution of fossil sources in BJ decreased by
577 about 6-15% for the different sampling season/period after the implementation of
578 Action Plan, based on previous studies (Fang et al., 2017; Lim et al., 2020; Liu et al.,
579 2016a, b; Ni et al., 2018, 2020; Shao et al., 1996; Sun et al., 2012; Yang et al., 2005;
580 Zhang et al., 2015, 2017a) and this study. Among them, fossil sources decreased
581 significantly in autumn and winter after the Action Plan, which were 15% and 14%,
582 respectively. The contribution of fossil sources in our study decreased by 16% in
583 winter compared with the previous results. For the polluted and clean periods, the
584 proportion of fossil sources reduced by 6% and 9%, respectively. With the
585 implementation of energy conservation and emission reduction policies, many
586 non-clean fossil fuels have been replaced by clean energy. In 2019, the coal

删除的内容: Figure 5

588 consumption in BJ was only 1.3 million tons, which was 91.5% lower than that in
 589 2013 (BJMBS, 2020).



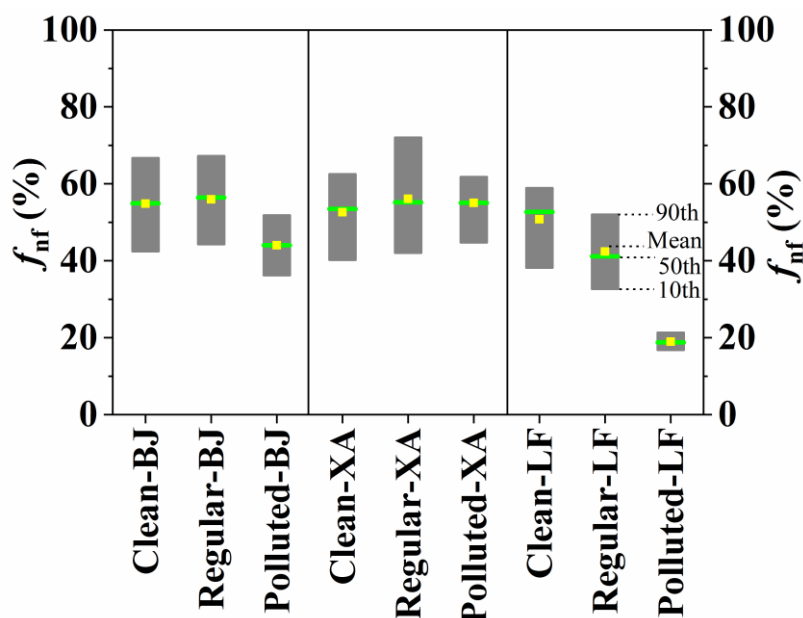
590
 591 Fig. 3 Variations in proportion of non-fossil sources (f_{nf}) of carbonaceous aerosols at
 592 the sampling sites in Beijing (BJ), Xi'an (XA), and Linfen (LF). The red scatter dot
 593 represents the f_{nf} of each sample, and the black solid line represents the sliding
 594 average f_{nf} value of every five samples (date, "yyymmdd").

595 Different from the results in BJ, the proportion of fossil sources in XA has not
 596 decreased significantly for each season/period (Fig. 5). This difference might be
 597 related with a small decline (< 0.5%) in coal consumption in Xi'an during 2019
 598 compared to 2013 (XAMBS, 2014, 2020). Due to the less attention to LF, there is still

删除的内容: lists the studies of ^{14}C in aerosols in our research area over the past few decades. With the progress of air quality management, the proportion of fossil sources decreased by 6–17% in BJ and XA (Huang et al., 2014; Lim et al., 2020; Liu et al., 2016; Ni et al., 2018, 2020; Shao et al., 1996; Sun et al., 2012; Yang et al., 2005; Zhang et al., 2015, 2017). With the implementation of energy conservation and emission reduction policies, many non-clean fossil fuels have been transformed into clean energy. In 2019, the coal consumption in BJ was only 1.3 million tons, which was 91.5% lower than that in 2013 (BJMBS, 2020).

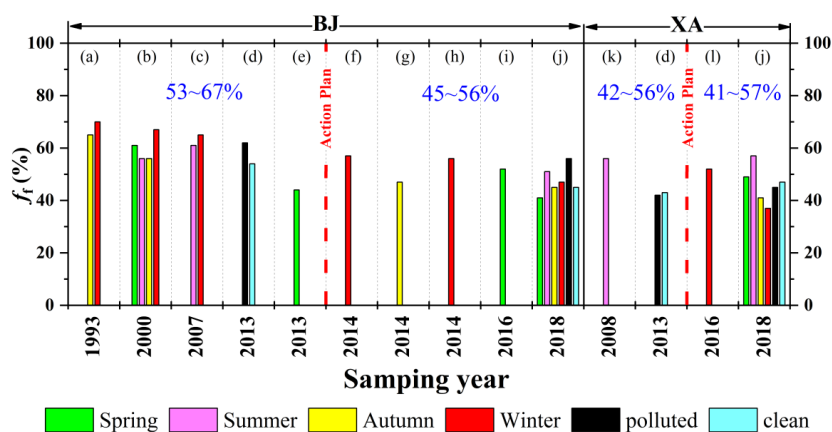
删除的内容: The decline in fossil source contributions in XA (6%) was smaller than that in BJ (17%) in the past few decades. This difference can be explained as follows: the decline in coal consumption in Shaanxi Province during 2019 was not significant compared to that in 2013, whereas the consumption of liquid fossil fuels decreased by 37% (SAPBS, 2020).

627 a lack of related research of carbonaceous aerosols using radiocarbon in this city to
 628 compare.



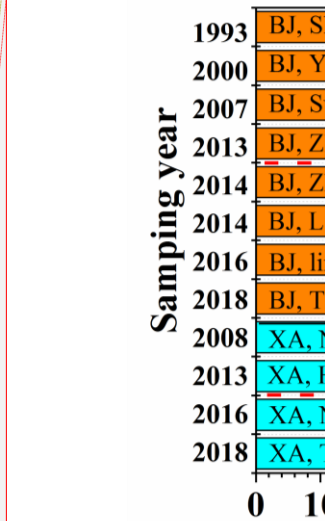
删除的内容: The particulate matter emitted from coal combustion is higher than that emitted from the combustion of liquid fossil fuels (Chen et al., 2005; England et al., 2002; Guo et al., 2014; Yan et al., 2010). Concerning non-fossil sources, China produces 939 million tons of agricultural biomass residues annually, which is the main energy source for some rural areas (Liao et al., 2004; Lu et al., 2009). In addition, the increase in urban vegetation coverage may also increase the photochemical reactions of biological volatile organic compounds (VOCs) (Gelencsér et al., 2007; NBS, 2021). Therefore, in recent years, non-fossil fuels have gradually become a major contributor to carbonaceous aerosols in BJ and XA with the reduction in the use of fossil energy. .

629
 630 Fig. 4 Boxplot distribution of f_{nf} of samples with different pollution levels. Clean
 631 samples: $PM_{2.5} < 75 \mu g m^{-3}$; regular samples: $75 \mu g m^{-3} \leq PM_{2.5} < 150 \mu g m^{-3}$;
 632 polluted samples: $PM_{2.5} \geq 150 \mu g m^{-3}$



删除的内容:
 带格式的: 字体: (默认) Times New Roman

633
 634 Fig. 5 Comparison of fossil proportion (f_i) of carbonaceous aerosol reported in
 635 different studies in Beijing (BJ) and Xi'an (XA), China for each season/period. The



删除的内容:
 带格式的: 字体: (默认) Times New Roman, 小四
 删除的内容: non-

660 data has been converted to the ratio of total carbon. The ranges shown in the upper
661 part of the figure are the average values of each season/period before and after the
662 Action Plan. (a) Shao et al., 1996; (b) Yang et al., 2005; (c) Sun et al., 2012; (d)
663 Zhang et al., 2015; (e) Liu et al., 2016b; (f) Zhang et al., 2017; (g) Liu et al., 2016a; (h)
664 Fang et al., 2017; (i) Lim et al., 2020; (j) This study; (k) Ni et al., 2018; (l) Ni et al.,
665 2021.
666

667 3.3 Air mass backward trajectory analysis

668 We analyzed and counted the backward trajectory during the sampling period;
669 several typical types were presented in Fig. S1. Figure S1 (a) shows the type of
670 backward trajectory with the highest frequency during the sample collection in BJ.
671 This type of long-distance transportation from the northwest accounted for
672 approximately 43.9% of all cases. The average PM_{2.5} concentration, carbonaceous
673 aerosol concentration, and f_{nf} of the sample were $45.4 \pm 22.7 \mu\text{g m}^{-3}$, $9.5 \pm 6.4 \mu\text{gC}$
674 m^{-3} , and $56 \pm 10\%$, respectively. As shown in Fig. S1 (b), when air mass was
675 transported from the south or stayed for a long time in the Hebei province, air
676 pollution was usually more serious. These cases accounted for approximately 26.3%
677 of all cases. The average concentrations of PM_{2.5} and carbonaceous aerosols were
678 $97.3 \pm 43.6 \mu\text{g m}^{-3}$ and $15.6 \pm 7.9 \mu\text{gC m}^{-3}$, which were 2.1 and 1.6 times of those in
679 the northwest, respectively. The aerosol concentration of air masses transported from
680 the southern region was higher than that from the northern regions. The f_{nf} value in
681 these cases was $46 \pm 5\%$, which was 10% higher than in the northwest cases. Thus, air
682 pollution in BJ might be affected by fossil sources in the Hebei province and other
683 southern regions.

删除的内容: 36

删除的内容: 3

删除的内容: 2

删除的内容: 0

删除的内容: 0

删除的内容: 1

删除的内容: 0

删除的内容: 4

692 The $PM_{2.5}$ and carbonaceous concentrations were low when the air mass
693 transported from the northwest for a long distance at the XA site (Fig. S1 (c)). In this
694 case, the average $PM_{2.5}$ concentration, carbonaceous aerosol concentration, and f_{nf} of
695 the samples were $93.1 \pm 65.1 \mu\text{g m}^{-3}$, $17.4 \pm 9.6 \mu\text{gC m}^{-3}$, and $62 \pm 7\%$, respectively.
696 However, when air masses circulated in the Guanzhong Basin or converged into the
697 basin from multiple directions due to the local topography (Fig. S1 (d)), the
698 concentration of carbonaceous aerosol was usually high. The proportion of this type
699 of air mass transportation accounted for 53.6% of the total cases. The average $PM_{2.5}$
700 concentration, carbonaceous aerosol concentration, and f_{nf} of the corresponding
701 samples were $132.0 \pm 72.8 \mu\text{g m}^{-3}$, $19.7 \pm 10.4 \mu\text{gC m}^{-3}$, and $58 \pm 9\%$, respectively.
702 Thus, air pollution in XA was mainly affected by the diffusion environment. The air
703 mass remained in the upper part of the Guanzhong region for a long time when the
704 diffusion environment was poor, causing secondary reactions and air pollution.
705 Moreover, when the air mass came from eastern cities (e.g., Henan or Hubei
706 provinces), f_{nf} was 47%, which was significantly lower than that in other cases. This
707 indicated that fossil source emissions in Henan and other eastern regions might
708 contribute to air pollution in XA.

709 As shown in Fig. S1 (e), when the air mass was long-distance transported to the
710 LF, the concentration of carbonaceous aerosols was relatively stable. However,
711 pollutants accumulated when the air mass returned over and around the city (Fig. S1
712 (f)). In these cases, the concentrations of $PM_{2.5}$ and carbonaceous aerosols of the
713 sample increased by 46.35–57.10%, and f_{nf} decreased by 5%. Thus, the LF samples
714 were more susceptible to the diffusion environment and the proportion of fossil
715 sources discharged locally.

删除的内容: was

删除的内容: 05

删除的内容: 37

删除的内容: 1

删除的内容: owing to topographical problems

删除的内容: 1.95

删除的内容: 75

删除的内容: 69

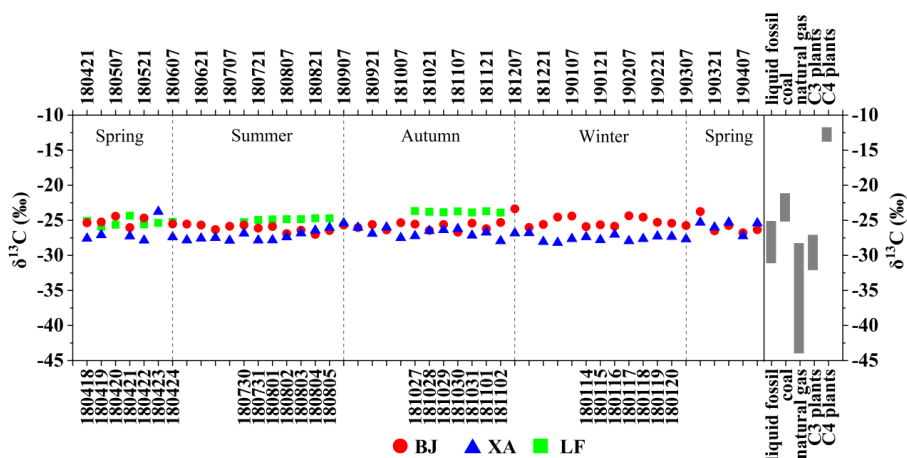
删除的内容: 3

726 Air pollution in BJ was more susceptible to the impact of transportation from the
 727 southern region, whereas XA and LF were more affected by local emissions and
 728 diffusion environments.

729

730 3.4 Best estimate of source apportionment of TC using ^{14}C and ^{13}C

731 The $\delta^{13}\text{C}$ values at the sampling sites in BJ, XA, and LF were $-25.65 \pm 0.79\text{‰}$,
 732 $-26.94 \pm 0.92\text{‰}$, and $-23.84 \pm 0.16\text{‰}$, respectively. Figure 6 shows the $\delta^{13}\text{C}$ values
 733 of the samples from each city and various sources. Specifically, $\delta^{13}\text{C}$ had lower values
 734 in the BJ and LF samples during summer ($-26.11 \pm 0.49\text{‰}$ and $-24.88 \pm 0.18\text{‰}$,
 735 respectively) and higher values during winter ($-25.07 \pm 0.79\text{‰}$ and $-23.84 \pm 0.16\text{‰}$,
 736 respectively). Conversely, the lower and higher $\delta^{13}\text{C}$ values in the XA samples
 737 appeared in winter ($-27.49 \pm 0.44\text{‰}$) and spring ($-26.34 \pm 1.23\text{‰}$).



738

739 Fig. 6 $\delta^{13}\text{C}$ values of samples from Beijing (BJ), Xi'an (XA), and Linfen (LF), and
 740 comparison with the $\delta^{13}\text{C}$ distribution of various sources. The abscissa represents the
 741 sampling date (yymmdd). The tick labels of top axis represent the date of BJ and XA,
 742 and the bottom represents the date of LF. The gray box indicates the $\delta^{13}\text{C}$ of the main
 743 source (Agnihotri et al., 2011; Huang et al., 2006; Lopez-Veneroni, 2009; Martinelli

- 删除的内容: 83
- 删除的内容: 81
- 删除的内容: 7.
- 删除的内容: 12
- 删除的内容: 91
- 删除的内容: 94
- 删除的内容: 32
- 删除的内容: 31
- 删除的内容: 25
- 删除的内容: 25
- 删除的内容: 25
- 删除的内容: 17
- 删除的内容: 94
- 删除的内容: 59
- 删除的内容: 3
- 删除的内容: 54

760 et al., 2002; Moura et al., 2008; [Pugliese et al., 2017](#); Smith & Epstein, 1971; [Vardag](#)
761 [et al., 2015](#); Widory, 2006).

762 Compared with the existing isotope indicators of various sources (Fig. 6), the
763 increase in $\delta^{13}\text{C}$ in the BJ and LF samples during winter may be more related to the
764 increase in coal combustion from local and the surrounding cities. The increase in
765 $\delta^{13}\text{C}$ in XA samples during autumn and winter may be related to the use of C4 plant
766 fuel, whereas the decrease during winter may be related to vehicle emissions and the
767 use of C3 plant fuels, such as wheat straw or wood.

768 ^{14}C and ^{13}C were used to quantify the sources of TC in the carbonaceous aerosols
769 (Fig. 7). For the carbonaceous aerosols in BJ and XA, the best estimate of source
770 apportionment showed that the contributions of liquid fossil fuels were $29.3 \pm 12.7\%$
771 and $24.9 \pm 18.0\%$, respectively, which were greater than the contribution of coal (15.5
772 $\pm 8.8\%$ and $20.9 \pm 14.2\%$, respectively). In 2019, coal accounted for only 2.6% of all
773 fossil fuels used in BJ (BJMBS, 2020). This indicates that the local combustion of
774 coal was very low, and the coal contribution might be somewhat related to
775 transportation from the surrounding regions. Moreover, the higher contribution of
776 liquid fossil fuels in BJ was due to the high number of motor vehicles (6.4 million),
777 which was 1.7 times higher than that in XA in 2019(BJMBS, 2020; XAMBS, 2020).
778 Figure S2 shows some studies on the source apportionment of coal and liquid fossil
779 fuels in aerosols in BJ over the past few decades. The coal contribution in BJ
780 decreased, whereas liquid fossil fuels gradually became the main source of fossil fuels.
781 After the implementation of the Action Plan, the proportion of coal in fossil sources
782 decreased by approximately 32% in BJ (Gao et al., 2018; Li et al., 2013; Liu et al.,
783 2014; Shang et al., 2019; Song et al., 2006; Tian et al., 2016; Wang et al., 2008;
784 Zhang et al., 2014).

删除的内容: Fig. 6 $\delta^{13}\text{C}$ values of samples from Beijing (BJ), Xi'an (XA), and Linfen (LF), and comparison with the $\delta^{13}\text{C}$ distribution of various sources. The abscissa represents the sampling date (yymmdd). The gray box indicates the $\delta^{13}\text{C}$ of the main source (Agnihotri et al., 2011; Huang et al., 2006; Lopez-Veneroni, 2009; Martinelli et al., 2002; Moura et al., 2008; Smith & Epstein, 1971; Widory, 2006).

删除的内容: 33.6

删除的内容: 9

删除的内容: 26

删除的内容: .6

删除的内容: 16

删除的内容: 4

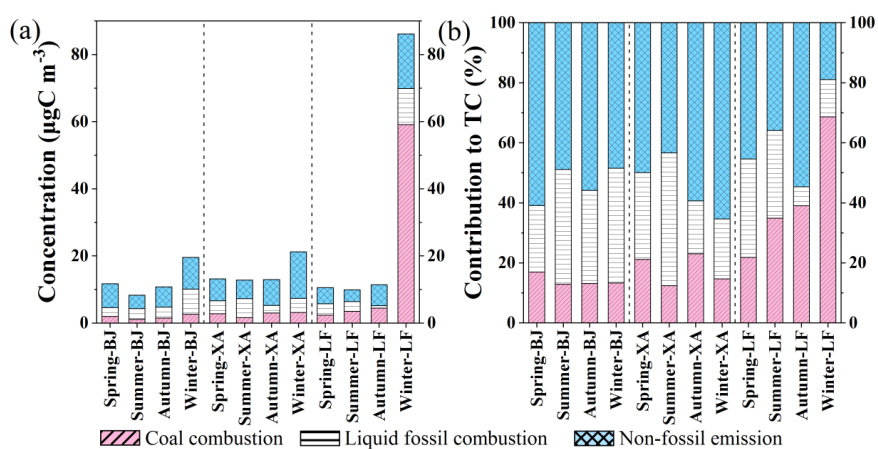
删除的内容: 11.2

删除的内容: 9.1

删除的内容: 19.2

删除的内容: 2.3

807 In contrast, coal combustion contributed $42.9 \pm 19.4\%$ to LF samples, which was
 808 greater than the contribution of liquid fossil emissions ($20.9 \pm 12.3\%$) and
 809 significantly higher than those in BJ and XA. Especially in winter, coal contributed as
 810 much as $68.6 \pm 3.6\%$ ($59.1 \pm 10.0 \mu\text{gC m}^{-3}$). According to the data released by the
 811 Shanxi Provincial Bureau of Statistics, coal consumption in Shanxi Province was as
 812 high as 349.06 million tons in 2019, which was 46.7 times of the consumption of
 813 liquid fossil fuels, accounting for 70.3% of the total fossil fuel consumption (SPBS,
 814 2020). The high contribution of coal combustion in winter might be related to the use
 815 of household coal for heating by rural residents in Shanxi. This is because household
 816 coal can emit a large amount of carbonaceous particles and is an important source of
 817 carbonaceous aerosols in rural areas in northern China (Chen et al., 2005; Shen et al.,
 818 2010; Streets et al., 2003a; Zhi et al., 2008).



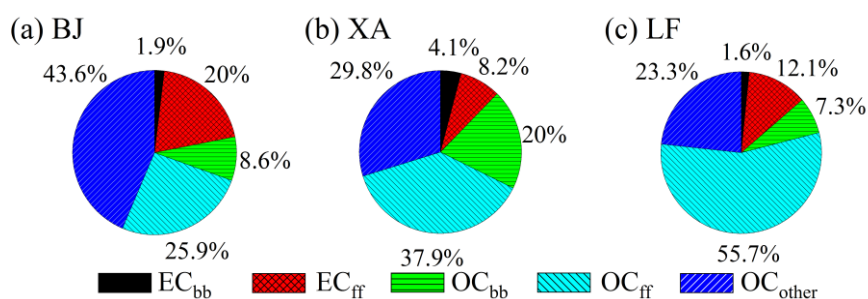
819 Fig. 7 Mass concentrations ($\mu\text{gC m}^{-3}$) (a) and percentage (b) of coal combustion,
 820 liquid fossil fuel, and non-fossil sources emissions for carbonaceous aerosols samples
 821 in Beijing (BJ), Xi'an (XA), and Linfen (LF) during different seasons.
 822 **3.5 Best estimate of source apportionment of OC and EC by ^{14}C and Lev**

删除的内容: 39.2
 删除的内容: 20.5
 删除的内容: 24.6
 删除的内容: 13.4

删除的内容: 6.2
 删除的内容: 7.
 删除的内容: 0
 删除的内容: 9.7

删除的内容: Source apportionment of
 删除的内容: using radiocarbon (^{14}C) and stable carbon (^{13}C) isotopes at the
 删除的内容: ing sit
 删除的内容: Red, blue, and orange represent the concentrations and contributions of coal combustion, liquid fossil fuel, and non-fossil sources emissions, respectively.

841 The concentration of each carbon component in BJ, XA, and LF was calculated
 842 based on the combination of Lev and ^{14}C . The best estimate of source apportionment
 843 showed in Fig. 8. The contributions of OC_{other} ($43.6 \pm 12.9\%$), OC_{ff} ($25.5 \pm 11.7\%$),
 844 and EC_{ff} ($20.5 \pm 6.5\%$) were relatively high in BJ. The OC_{bb} ($23.0 \pm 17.3\%$) and OC_{ff}
 845 ($39.7 \pm 9.7\%$) were the highest contributors in XA. The LF samples showed different
 846 characteristics, and the contribution of fossil sources was significantly high, especially
 847 for the OC_{ff} ($56.1 \pm 11.9\%$).



848 Fig. 8 Percentage of elemental carbon from biomass burning (EC_{bb}) and fossil-fuel
 849 combustion (EC_{ff}) and percentage of organic carbon from biomass burning (OC_{bb}),
 850 combustion (EC_{ff}) and percentage of organic carbon from biomass burning (OC_{bb}),
 851 fossil-fuel combustion (OC_{ff}), and other sources (OC_{other}) for the $\text{PM}_{2.5}$ samples in
 852 Beijing (BJ), Xi'an (XA), and Linfen (LF).

853 3.5.1 Biomass burning contribution to TC

854 The concentrations ($0.3 \pm 0.3 \mu\text{gC m}^{-3}$) and contributions ($1.9 \pm 1.4\%$) of EC_{bb} in
 855 BJ were relatively low during the whole year (Fig. 9). The EC_{bb} at the XA and LF
 856 sites had high concentrations in autumn ($0.7 \pm 0.5 \mu\text{gC m}^{-3}$ and $0.6 \pm 0.1 \mu\text{gC m}^{-3}$) and
 857 winter ($1.5 \pm 0.7 \mu\text{gC m}^{-3}$ and $1.7 \pm 0.3 \mu\text{gC m}^{-3}$) and low concentrations in summer
 858 ($0.2 \pm 0.1 \mu\text{gC m}^{-3}$ and $0.1 \pm 0.0 \mu\text{gC m}^{-3}$), respectively. The OC_{bb} concentrations in
 859 the BJ, XA, and LF samples showed an increase in autumn ($1.6 \pm 1.4 \mu\text{gC m}^{-3}$, $3.3 \pm$
 860 $2.2 \mu\text{gC m}^{-3}$, and $2.9 \pm 0.4 \mu\text{gC m}^{-3}$) and winter ($2.5 \pm 2.1 \mu\text{gC m}^{-3}$, $6.9 \pm 3.3 \mu\text{gC m}^{-3}$,
 861 and $7.9 \pm 1.3 \mu\text{gC m}^{-3}$), respectively. Especially in the XA samples, OC_{bb} had high

- 删除的内容: 22
- 删除的内容: 27
- 删除的内容: 4
- 删除的内容: 1
- 删除的内容: 62
- 删除的内容: 42
- 删除的内容: 58
- 删除的内容: 09
- 删除的内容: 35
- 删除的内容: 60
- 删除的内容: 53
- 删除的内容: 21
- 删除的内容: 12
- 删除的内容: 05
- 删除的内容: 05
- 删除的内容: 02
- 删除的内容: 73
- 删除的内容: 57
- 删除的内容: 97
- 删除的内容: 62
- 删除的内容: 3.63
- 删除的内容: 55
- 删除的内容: 75
- 删除的内容: 33
- 删除的内容: 8.72
- 删除的内容: 91
- 删除的内容: 9.57
- 删除的内容: 33

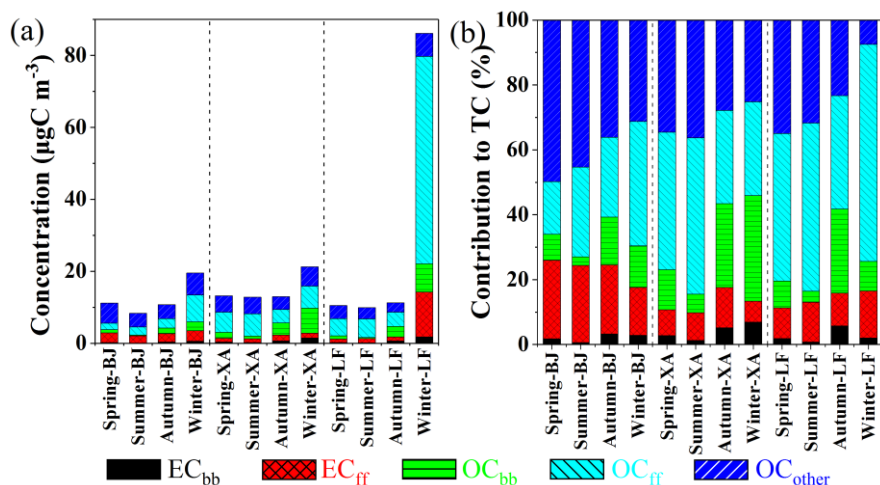
890 contributions in autumn ($28.6 \pm 15.8\%$) and winter ($32.8 \pm 12.3\%$). The contribution
891 of biomass combustion in XA ($24.1 \pm 18.0\%$) was significantly larger than that in BJ
892 ($10.8 \pm 7.9\%$) and LF ($8.8 \pm 8.9\%$), which was also reflected in the concentration of
893 Lev (Fig. S3). The Lev concentration in XA ($0.36 \pm 0.38 \mu\text{g m}^{-3}$) was higher than that
894 in BJ ($0.15 \pm 0.17 \mu\text{g m}^{-3}$) and slightly higher than that in LF ($0.32 \pm 0.34 \mu\text{g m}^{-3}$).
895 Furthermore, the Lev concentration in XA during autumn and winter was up to 5.3
896 times higher than that during the other seasons. Especially in winter, the proportion of
897 Lev in the TC was $4.0 \pm 2.3\%$ in XA, which was 3.9 and 3.8 times those in BJ and LF,
898 respectively. Zhang et al. (2015) attributed this to emissions from neighboring rural
899 regions because such areas use biofuels for heating and cooking more commonly in
900 winter. China produces 939 million tons of agricultural biomass residues annually,
901 which is the main energy source for some rural areas (Liao et al., 2004; Lu et al.,
902 2009). In addition, the increase in urban vegetation coverage may also increase the
903 photochemical reactions of biological volatile organic compounds (VOCs) (Gelencsér
904 et al., 2007; NBS, 2021). Therefore, in recent years, non-fossil fuels have gradually
905 become a major contributor to carbonaceous aerosols in BJ and XA with the reduction
906 in the use of fossil energy.

- 删除的内容: 32.4
- 删除的内容: 13
- 删除的内容: 9
- 删除的内容: 40.7
- 删除的内容: 4
- 删除的内容: 6.5
- 删除的内容: 9.9
- 删除的内容: 4
- 删除的内容: 8.3
- 删除的内容: 9.0
- 删除的内容: 11.0
- 删除的内容: 35
- 删除的内容: 40
- 删除的内容: 11
- 删除的内容: 14
- 删除的内容: 31
- 删除的内容: 33
- 删除的内容: 6.1
- 删除的内容: 2
- 删除的内容: 0
- 删除的内容: 7
- 删除的内容: 4.5

907 3.5.2 Fossil contribution to TC

908 The EC_{ff} concentrations at BJ (spring: $2.7 \pm 1.4 \mu\text{gC m}^{-3}$; summer: $2.0 \pm 0.8 \mu\text{gC}$
909 m^{-3} ; autumn: $2.3 \pm 2.0 \mu\text{gC m}^{-3}$; winter: $2.9 \pm 2.6 \mu\text{gC m}^{-3}$) and XA (spring: 1.1 ± 0.8
910 $\mu\text{gC m}^{-3}$; summer: $1.1 \pm 1.1 \mu\text{gC m}^{-3}$; autumn: $1.6 \pm 2.3 \mu\text{gC m}^{-3}$; winter: 1.4 ± 0.8
911 $\mu\text{gC m}^{-3}$) did not fluctuate significantly during the year. The concentration of EC_{ff} in
912 LF during spring, summer, and autumn was relatively stable (1.0 – $1.2 \mu\text{gC m}^{-3}$), but it
913 was high during winter ($12.5 \pm 2.5 \mu\text{gC m}^{-3}$), reaching 10.2 times that in summer.

- 删除的内容: 76
- 删除的内容: 41
- 删除的内容: 1.99
- 删除的内容: 4
- 删除的内容: 36
- 删除的内容: 2.00
- 删除的内容: 3.00
- 删除的内容: 72
- 删除的内容: 14
- 删除的内容: 73
- 删除的内容: 4
- 删除的内容: 06
- 删除的内容: 66
- 删除的内容: 32
- 删除的内容: 48
- 删除的内容: 73
- 删除的内容: 1.05
- 删除的内容: 24
- 删除的内容: 66
- 删除的内容: 50



956 Fig. 9 Mass concentrations ($\mu\text{gC m}^{-3}$) (a) and percentage (b) of elemental carbon from
 957 biomass burning (EC_{bb}) and fossil-fuel combustion (EC_{ff}), organic carbon from
 958 biomass burning (OC_{bb}), fossil-fuel combustion (OC_{ff}), and other sources (OC_{other}) for
 959 carbonaceous aerosols samples in Beijing (BJ), Xi'an (XA), and Linfen (LF) during
 960 different seasons.
 961

962 The concentration of OC_{ff} was slightly higher in XA during summer (6.2 ± 2.2
 963 $\mu\text{gC m}^{-3}$) and winter ($6.1 \pm 2.1 \mu\text{gC m}^{-3}$). The contribution of OC_{ff} in the BJ samples
 964 increased to $32.4 \pm 14.5\%$ during winter and decreased to $18.4 \pm 8.4\%$ during spring.
 965 The $\text{OC}_{\text{ff}}/\text{EC}_{\text{ff}}$ ratios in BJ and LF during winter were approximately 2.3 ± 1.2 and 4.7
 966 ± 0.7 , respectively, suggesting that the fossil source secondary carbonaceous aerosols
 967 were higher in winter. This can be explained by the lower temperature in the winter
 968 altering the gas-particle equilibrium, suggesting that a larger portion of the OC_{ff}
 969 during winter was secondary aerosol (Genberg et al., 2011). OC_{ff} in LF had high
 970 concentrations in winter ($57.6 \pm 9.2 \mu\text{gC m}^{-3}$) and low concentrations in summer (5.2
 971 $\pm 1.2 \mu\text{gC m}^{-3}$). This indicated that the burning of fossil sources was an important
 972 source of OC in BJ (OC_{ff} : $32.4 \pm 14.5\%$) and LF (OC_{ff} : $66.8 \pm 1.7\%$) during winter.
 973 Fang et al. (2017) found that fossil fuels contributed significantly ($> 50\%$) to carbon

删除的内容: 20

删除的内容: 20

删除的内容: 88

删除的内容: 38

删除的内容: 31.9

删除的内容: 6

删除的内容: 7.8

删除的内容: 2

删除的内容: 8.29

删除的内容: 34

删除的内容: 15

删除的内容: 3

删除的内容: 31.9

删除的内容: 6

删除的内容: 7.6

删除的内容: 8

990 components in the haze in East Asia during January 2014, suggesting that the aerosol
991 contribution was generally dominated by fossil combustion sources. Therefore, using
992 cleaner energy and cleaner residential stoves to reduce and replace the high-emission
993 end-use coal combustion processes and control the emissions from liquid-fossil-fueled
994 vehicles in megacities should be beneficial to the air quality.

995 3.5.3 Other non-fossil contributions to OC

996 In addition to the OC directly emitted from fossil and biomass fuels, there are
997 many components of OC, such as SOC, whose source is difficult to identify.
998 Residential oil fume emissions from urban residents, emissions from biological
999 sources, and secondary bio-organic aerosols generated by the secondary reaction of
1000 biomass fuels are also important components of OC (Gelencs é et al., 2007; Zhang et
1001 al., 2015).

1002 The concentration of OC_{other} in the LF samples did not vary greatly during spring
1003 (~~3.7 ± 1.2~~ $\mu\text{gC m}^{-3}$) and summer (~~3.2 ± 0.5~~ $\mu\text{gC m}^{-3}$), but it was lower in autumn (~~2.6 ±~~
1004 ~~0.3~~ $\mu\text{gC m}^{-3}$) and higher in winter (~~6.5 ± 2.8~~ $\mu\text{gC m}^{-3}$). In BJ, the contribution of
1005 OC_{other} was high during spring (~~49.9 ± 9.9~~%) and summer (~~45.8 ± 9.8~~ %), and its
1006 concentration was relatively high during winter (~~6.1 ± 5.6~~ $\mu\text{gC m}^{-3}$). Zhang et al.
1007 (2015) mainly attributed the presence of OC_{other} in northern China to SOC formation
1008 from non-fossil, non-biogenic precursors. In general, secondary bio-organic aerosols
1009 in spring and autumn are mainly caused by biological emissions or long-distance
1010 transportation of biological VOCs and secondary organic aerosols (SOAs) in
1011 particulates (Gelencs é et al., 2007; Jimenez et al., 2009). The high concentration in
1012 winter may be because low temperatures drive condensable semi-volatile organic
1013 compounds (SVOCs) into the particulate phase (Simpson et al., 2007; Tanarit et al.,
1014 2008).

- 删除的内容: 74
- 删除的内容: 19
- 删除的内容:),
- 删除的内容: 17
- 删除的内容: 53
- 删除的内容: , and winter ($4.06 \pm 2.55 \mu\text{gC m}^{-3}$),
- 删除的内容: 1.61
- 删除的内容: 20
- 删除的内容: 51
- 删除的内容: .0
- 删除的内容: 3
- 删除的内容: 5.96
- 删除的内容: 48

1029 The OC_{other} contribution and concentration in XA were high in summer ($35.2 \pm$
1030 10.0%) and winter ($5.4 \pm 4.2 \mu\text{C m}^{-3}$), respectively. We assume that this excess is
1031 mainly attributed to SOC formation from non-fossil and primary biogenic particles.
1032 Some SOAs are formed by VOCs that are produced by burning wood or biofuels (e.g.,
1033 ethanol), and they increase the load of these sources on organic aerosols (Genberg et
1034 al., 2011). Huang et al. (2014) found that severe haze pollution was largely driven by
1035 secondary aerosol formation, and non-fossil SOAs dominated, accounting for $66 \pm 8\%$
1036 of the SOAs in XA despite extensive urban emissions. Ni et al. (2020) also considered
1037 that non-fossil sources largely contributed (56%) to SOC in XA. Thus, the control of
1038 biomass burning activities could be an efficient strategy for reducing aerosols,
1039 especially in XA. Furthermore, SOC formation from these non-fossil VOCs may be
1040 enhanced when they are mixed with other pollutants, such as VOCs and NO_x (Hoyle
1041 et al., 2011; Weber et al., 2007). Motor vehicles are one of the main anthropogenic
1042 sources of VOCs and NO_x (Barletta et al., 2005; Liu et al., 2008). In Section 3.4, we
1043 found that the carbonaceous concentrations from motor vehicle emissions were high
1044 in XA during winter and summer (Fig. 7a), and the increasing of motor vehicle
1045 activities might partly explain the high concentration of OC_{other} during the two
1046 seasons.

删除的内容: The OC_{other} contributions in XA were high in spring ($33.9 \pm 7.5\%$) and summer ($34.9 \pm 10.1\%$).

已下移 [2]: Furthermore, SOC formation from these non-fossil VOCs may be enhanced when they are mixed with other pollutants, such as VOCs and NO_x (Hoyle et al., 2011; Weber et al., 2007). Motor vehicles are one of the main anthropogenic sources of VOCs and NO_x (Barletta et al., 2005; Liu et al., 2008). We found that motor vehicle emissions were higher in BJ and XA during winter and summer, respectively (Fig. 7), which might explain the high concentration of OC_{other} in BJ during winter and in XA during summer.

已移动(插入) [2]

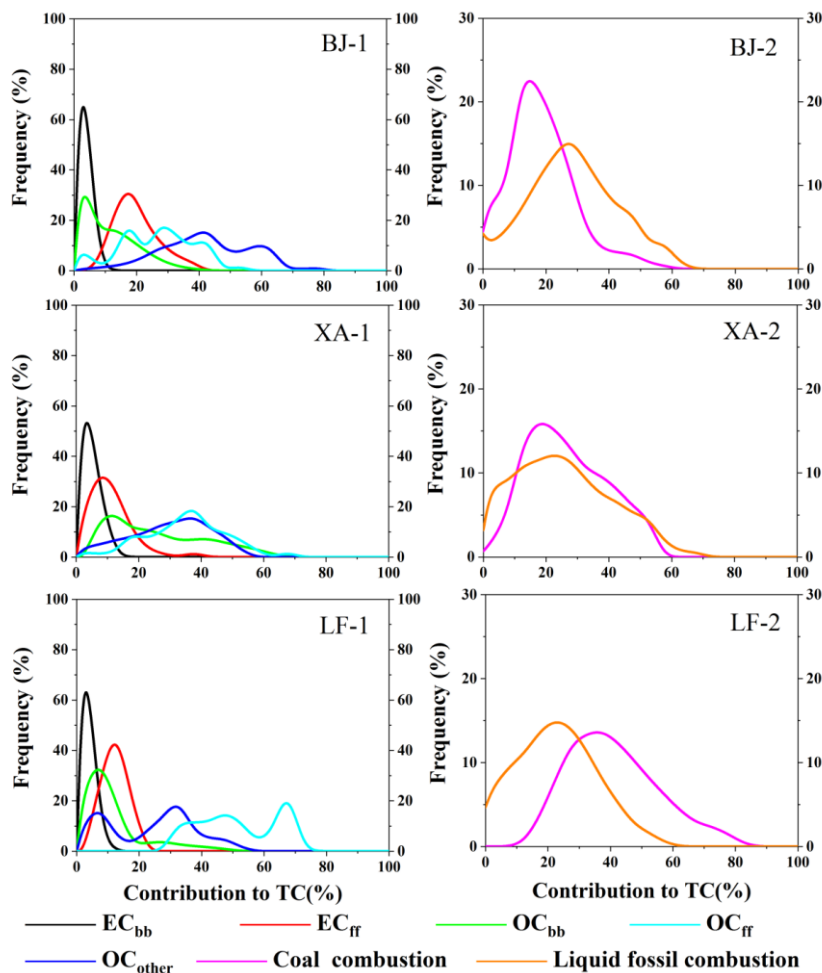
删除的内容: Furthermore, SOC formation from these non-fossil VOCs may be enhanced when they are mixed with other pollutants, such as VOCs and NO_x (Hoyle et al., 2011; Weber et al., 2007). Motor vehicles are one of the main anthropogenic sources of VOCs and NO_x (Barletta et al., 2005; Liu et al., 2008).

删除的内容: We found that motor vehicle emissions were higher in BJ and XA during winter and summer, respectively (Fig. 7), which might explain the high concentration of OC_{other} in BJ during winter and in XA during summer.

1048 3.6 Uncertainty analysis

1049 The results of the uncertainty analysis of the given set (Table 1) of the
1050 parameters in the three cities were shown in Fig. 10. Each curve represents the
1051 probability distribution of the sources of carbon components that contribute to the TC,
1052 from which the uncertainty of the source allocation can be derived. Some results were
1053 uncertain because the input parameters of the LHS calculation varied greatly. The

1088 contributions of OC_{fr} and OC_{other} to the TC were mostly uncertain. This is mainly
 1089 related to the uncertainty of the two parameters, Lev/OC_{bb} and $(EC/OC)_{bb}$. Both these
 1090 parameters depend on the burning conditions and type of biomass, as mentioned in
 1091 Section 2.9. More reliable data would be obtained if $^{13}C/^{14}C$ could be performed on
 1092 the pure OC fractions of the samples, which has been proven to be feasible (Huang et
 1093 al., 2014; Szidat et al., 2004, 2006; Zhang et al., 2015). Other contributions have
 1094 single peaks, which prove that the results of the source analysis are reliable. These
 1095 results demonstrate that we can identify the main contributors.



带格式的: 字体: (默认) Times
New Roman, 四号, 加粗

1096

1097 Fig. 10 Latin hypercube sampling of frequency distributions of the source
1098 contributions to total carbon (TC) from fossil, organic carbon (OC), and elemental
1099 carbon (EC) source categories (Table 1) for the samples collected in Beijing (BJ),
1100 Xi'an (XA), and Linfen (LF).

1101

1102 4 Conclusions

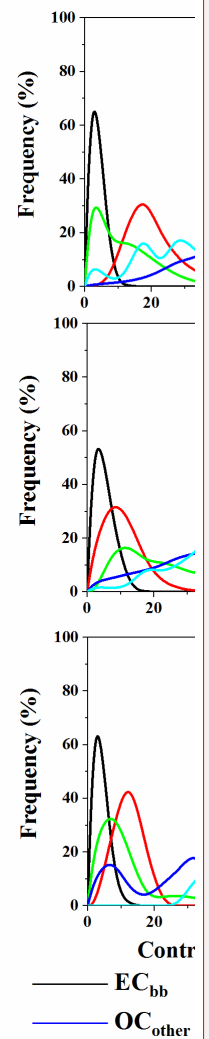
1103 PM_{2.5} samples were collected from BJ, XA, and LF in northern China from
1104 January 2018 to April 2019. The main objective of this study was to quantify the
1105 sources of carbonaceous aerosols by measuring the EC, OC, Lev, ¹³C, and ¹⁴C
1106 combined with LHS.

1107 The TC accounted for approximately 17.5 ± 6%, 21.5 ± 21%, and 17.8 ± 7.2% of
1108 PM_{2.5} in the samples from BJ, XA, and LF, and the corresponding concentrations
1109 were 12.5 ± 11.8 μgC m⁻³, 14.6 ± 7.5 μgC m⁻³, and 35.7 ± 36.5 μgC m⁻³, respectively.

1110 The concentrations at the three sites showed high values in winter and low values in
1111 summer. Based on backward trajectory analysis, we found that carbonaceous aerosols
1112 in BJ were more susceptible to transportation from the southern regions. Local
1113 emissions and the diffusion environment significantly impacted carbonaceous
1114 aerosols in XA and LF.

1115 The best estimate of source apportionment of the fossil components in the TC
1116 showed that the contribution of liquid fossil fuel combustion was 29.3 ± 12.7% and
1117 24.9 ± 18.0% in BJ and XA, respectively, which was greater than the contribution of
1118 coal combustion (15.5 ± 8.8%; 20.9 ± 14.5%). In contrast, coal combustion
1119 contributed 42.9 ± 19.4% in LF, which was greater than the contribution of liquid
1120 fossil fuel combustion (20.9 ± 12.3%).

1121 The best estimate of source apportionment of OC and EC indicated that the



删除的内容:

带格式的: 字体: (默认) Times New Roman, 四号, 加粗

删除的内容: 10

删除的内容: 0...±11.79... μgC m⁻³

删除的内容: 33.6...9.3 ± 12.9...%

1146 contributions of EC_{ff} (20.0 ± 6.5%), OC_{ff} (25.9 ± 11.6%), and OC_{other} (43.6 ± 12.9%)
1147 were relatively high in BJ. The OC_{ff} contribution was higher in winter (32.4 ± 14.5%),
1148 and its concentration was 3.3 times higher than that in other seasons. The contribution
1149 of OC_{bb} (20.0 ± 15.3%) and OC_{ff} (37.9 ± 10.8%) was higher in XA. The contribution
1150 of biomass burning to the TC was as high as 39.6 ± 14.5% in winter. The contribution
1151 of OC_{ff} in LF was significantly high (55.7 ± 12.2%), especially in winter (66.8 ±
1152 1.7%).

1153 The decline (6–16%) in the contribution of fossil sources since the
1154 implementation of the Action Plan indicates the effectiveness of air quality
1155 management. In the future, the government needs to further regulate and control
1156 emissions from motor vehicles in megacities such as BJ and XA. The cleaner use of
1157 coal must be further strengthened in coal-based cities such as LF in the eastern part of
1158 the Fenwei Plain. This study indicates that attention should be paid to the control of
1159 biomass burning in northern China, especially in the Guanzhong region.

1160

1161 **Code and data availability:** The data products in this paper are available at the East
1162 Asian Paleoenvironmental Science Database, National Earth System Science Data
1163 Center, National Science & Technology Infrastructure of China
1164 (http://paleodata.ieecas.cn/index_EN.aspx).

1165

1166 **Author contributions:** HZ performed the data analysis and wrote the initial draft of
1167 the manuscript. ZN and WZ conceived the project and reviewed the paper. ZN and
1168 SW provided the samples. HZ, XF, SW, XL and HD conducted the measurements. All
1169 authors made substantial contributions to this work.

1170

- 删除的内容: 5
- 删除的内容: 7.8
- 删除的内容: 7
- 删除的内容: 1.9
- 删除的内容: 6
- 删除的内容: 4
- 删除的内容: 3.0
- 删除的内容: 7.3
- 删除的内容: 9.7
- 删除的内容: %
- 删除的内容: 9.7
- 删除的内容: 46.94
- 删除的内容: 14
- 删除的内容: 56.1
- 删除的内容: 11.9
- 删除的内容: 7.6
- 删除的内容: 8
- 删除的内容: 17

1189 **Competing interests:** The authors declare that they have no conflict of interest.

1190

1191 **Acknowledgments:** The authors acknowledge the help of anonymous reviewers for
1192 improving this article.

1193

1194 **Financial support:** The study was financially supported by the Strategic Priority
1195 Research Program of the Chinese Academy of Sciences (XDA23010302), National
1196 Research Program for Key Issues in Air Pollution Control (DQGG0105-02), the
1197 National Natural Science Foundation of China (41730108, 42173082, and 41773141),
1198 Natural Science Foundation of Shaanxi province (2014JQ2-4018), Key projects of
1199 CAS (ZDRW-ZS-2017-6), and Natural Science Basic Research Program of Shaanxi
1200 Province (2019JCW-20).

1201

1202 **References**

1203 Aggarwal, S. G., and Kawamura, K.: Molecular distributions and stable carbon
1204 isotopic compositions of dicarboxylic acids and related compounds in aerosols
1205 from Sapporo, Japan: Implications for photochemical aging during long-range
1206 atmospheric transport, *J. Geophys. Res.*, 113, D14301,
1207 <https://doi.org/10.1029/2007JD009365>, 2008.

1208 Agnihotri, R., Mandal, T. K., Karapurkar, S. G., Naja, M., Gadi, R., Ahammed, Y.
1209 N., Kumar, A., Saud, T., and Saxena, M.: Stable carbon and nitrogen isotopic
1210 composition of bulk aerosols over India and northern Indian Ocean, *Atmos.*
1211 *Environ.*, 45, 2828-2835, <https://doi.org/10.1016/j.atmosenv.2011.03.003>, 2011.

1212 Andersson, A., Deng, J. J., Du, K., Zheng, M., Yan, C. Q., Sköld, M., and Gustafsson,
1213 O. r.: Regionally-varying combustion sources of the January 2013 severe haze

1214 events over eastern China, *Environ. Sci. Technol.*, 49, 2038-2043,
1215 <https://doi.org/10.1021/es503855e>, 2015.

1216 Bachar, A., Markus-Shi, J., Regev, L., Boaretto, E., and T. Klein, T.: Tree rings reveal
1217 the adverse effect of water pumping on protected riparian *Platanus orientalis* tree
1218 growth, *For. Ecol. Manag.*, 458, 0378-1127,
1219 <https://doi.org/10.1016/j.foreco.2019.117784>, 2020.

1220 Barletta, B., Meinardi, S., Rowland, F. S., Chan, C., Wang, X. M., Zou, S. C., Chan,
1221 L., and Blake, D. R.: Volatile organic compounds in 43 Chinese cities, *Atmos.*
1222 *Environ.*, 39, 5979-5990, <https://doi.org/10.1016/j.atmosenv.2005.06.029>, 2005.

1223 BJMBS: (Beijing Municipal Bureau Statistics): Beijing Statistical Yearbook-2020,
1224 China Statistics press.,
1225 <http://nj.tjj.beijing.gov.cn/nj/main/2020-tjnj/zk/indexch.htm>, 2020 (last access:
1226 28 March 2022).

1227 Cachier, H., Buat Menard, P., Fontugne, M., and Rancher, J.: Source terms and source
1228 strengths of the carbonaceous aerosol in the tropics, *J. Atmos. Chem.*, 3, 469-489,
1229 <https://doi.org/10.1007/BF00053872>, 1985.

1230 Cachier, H., Buat Menard, P., Fontugne, M., and Chesselet, R.: Long-range transport
1231 of continentally-derived particulate carbon in the marine atmosphere: Evidence
1232 from stable carbon isotope studies, *Tellus B*, 38, 161-177,
1233 <https://doi.org/10.1111/j.1600-0889.1986.tb00184.x>, 1986.

1234 Cao, J. J., Lee, S. C., Ho, K. F., Zhang, X. Y., Zou, S. C., Fung, K., Chow, J. C., and
1235 Watson, J. G.: Characteristics of carbonaceous aerosol in Pearl River Delta
1236 Region, China during 2001 winter period, *Atmos. Environ.*, 37, 1451-1460,
1237 [https://doi.org/10.1016/S1352-2310\(02\)01002-6](https://doi.org/10.1016/S1352-2310(02)01002-6), 2003.

1238 Cao, J. J., Lee, S. C., Chow, J. C., Watson, J. G., Ho, K. F., Zhang, R. J., Jin, Z. D.,

1239 Shen, Z. X., Chen, G. C., and Kang, Y. M.: Spatial and seasonal distributions of
1240 carbonaceous aerosols over China, *Journal of Geophysical Research*
1241 *Atmospheres*, D112, 22-11, <https://doi.org/10.1029/2006JD008205>, 2007.

1242 Cao, J. J., Zhu, C. S., Chow, J. C., Watson, J. G., Han, Y. M., Wang, G. H., Shen, Z. X.,
1243 and An, Z. S.: Black carbon relationships with emissions and meteorology in
1244 Xi'an, China, *Atmos. Res.*, 94, 194-202, <https://doi.org/10.1029/2006JD008205>,
1245 2009.

1246 Cao, J. J., Chow, J. C., Tao, J., Lee, S. C., Watson, J. G., Ho, K., Wang, G. H., Zhu, C.
1247 S., and Han, Y. M.: Stable carbon isotopes in aerosols from Chinese cities:
1248 Influence of fossil fuels, *Atmos. Environ.*,
1249 <https://doi.org/10.1016/j.atmosenv.2010.10.056>, 2011.

1250 Cao, J. J., Shen, Z. X., Chow, J. C., Watson, J. G., Lee, S. C., Tie, X. X., Ho, K. F.,
1251 Wang, G. H., and Han, Y. M.: Winter and summer PM_{2.5} chemical compositions
1252 in fourteen Chinese Cities, *Air Waste Manage Assoc*, 62, 1214–1226,
1253 <https://doi.org/10.1080/10962247.2012.701193>, 2012.

1254 Castro, L. M., Pio, C. A., Harrison, R. M., and Smith, D.: Carbonaceous aerosol in
1255 urban and rural European atmospheres: estimation of secondary organic carbon
1256 concentrations, *Atmos. Environ.*, 33, 2771-2781,
1257 <https://doi.org/10.1111/j.1553-2712.2005.tb00860.x>, 1999.

1258 Ceburnis, D., Garbaras, A., Szidat, S., Rinaldi, M., Fahrmi, S., Perron, N., Wacker, L.,
1259 Leinert, S., Remeikis, V., Facchini, M. C., Prevot, A. S. H., Jennings, S. G., and
1260 O'Dowd, C. D.: Quantification of the carbonaceous matter origin in submicron
1261 marine aerosol particles by dual carbon isotope analysis, *Atmos. Chem. Phys.*
1262 *Discuss.*, 11, 8593-8606, <https://doi.org/10.5194/acpd-11-2749-2011>, 2011.

1263 Chen, Y. J., Sheng, G. Y., Bi, X. H., Feng, Y. L., Mai, B. X., and Fu, J. M.: Emission

1264 Factors for Carbonaceous Particles and Polycyclic Aromatic Hydrocarbons from
1265 Residential Coal Combustion in China, *Environ. Sci. Technol.*, 39, 1861-1867,
1266 <https://doi.org/10.1021/es0493650>, 2005.

1267 Chesselet, R., Fontugne, M., Buat Menard, P., Ezat, U., and Lambert, C. E.: The
1268 origin of particulate organic carbon in the marine atmosphere as indicated by its
1269 stable carbon isotopic composition, *Geophys. Res. Lett.*, 8, 345-348,
1270 <https://doi.org/10.1029/GL008i004p00345>, 1981.

1271 Chow, J. C., and Watson, J. G.: PM_{2.5} carbonate concentrations at regionally
1272 representative Interagency Monitoring of Protected Visual Environment sites,
1273 *Journal of Geophysical Research Atmospheres*, 107,
1274 <https://doi.org/10.1029/2001JD000574>, 2002.

1275 Chow, J. C., Watson, J. G., Chen, L. W. A., Arnott, W. P., Moosmüller, H., and Fung,
1276 K.: Equivalence of Elemental Carbon by Thermal/Optical Reflectance and
1277 Transmittance with Different Temperature Protocols, *Environ. Sci. Technol.*, 38,
1278 4414-4422, <https://doi.org/10.1021/es034936u>, 2004.

1279 Claeys, M., Kourtchev, I., Pashynska, V., Vas, G., Vermeylen, R., Wang, W., Cafmeyer,
1280 J., Chi, X., Artaxo, P., Andreae, M. O., and Maenhaut, W.: Polar organic marker
1281 compounds in atmospheric aerosols during the LBA-SMOCC 2002 biomass
1282 burning experiment in Rondônia, Brazil: sources and source processes, time
1283 series, diel variations and size distributions, *Atmos. Chem. Phys.*,
1284 <https://doi.org/10.5194/acp-10-9319-2010>, 2010.

1285 Clarke, A. G., and Karani, G. N.: Characterisation of the carbonate content of
1286 atmospheric aerosols, *J. Atmos. Chem.*, 14, 119-128,
1287 <https://doi.org/10.1007/BF00115228>, 1992.

1288 Clayton, G. D., Arnold, J. R., and Patty, F. A.: Determination of Sources of Particulate

1289 Atmospheric Carbon, Science, 122, 751-753,
1290 <https://doi.org/10.1126/science.122.3173.751>, 1955.

1291 Coplen, T. B.: New guidelines for reporting stable hydrogen, carbon, and oxygen
1292 isotope-ratio data, *Geochim. Cosmochim. Acta*, 60, 3359-3360,
1293 [https://doi.org/10.1016/0016-7037\(96\)00263-3](https://doi.org/10.1016/0016-7037(96)00263-3), 1996.

1294 CSC: (Chinese State Council): Action Plan for Air Pollution Prevention and Control,
1295 http://www.gov.cn/zhengce/content/2013-09/13/content_4561.htm, 2013 (last
1296 access: 28 March 2022).

1297 CSC: (Chinese State Council): Three-year action plan to fight air pollution (NO. 2018.
1298 22), http://www.gov.cn/zhengce/content/2018-07/03/content_5303158.htm, 2018
1299 (last access: 28 March 2022).

1300 Currie, L. A.: Evolution and Multidisciplinary Frontiers of ¹⁴C Aerosol Science,
1301 *Radiocarbon*, 42, 115-126, <https://doi.org/10.1017/S003382220005308X>, 2000.

1302 Draxler, R. R., and Hess, G. D.: An overview of the HYSPLIT_4 modelling system
1303 for trajectories, dispersion and deposition, *Aust. Meteorol. Mag.*, 47, 295-308,
1304 1998.

1305 England, G., Chang, O., and Wien, S.: Development of fine particulate emission
1306 factors and speciation profiles for oil and gas-fired combustion systems, United
1307 States, 2002.

1308 Engling, G., Carrico, C. M., Kreidenweis, S. M., Collett Jr., J. L., Day, D. E., Malm, W.
1309 C., Lincoln, E., Hao, W. M., Iinuma, Y., and Herrmann, H.: Determination of
1310 levoglucosan in biomass combustion aerosol by high-performance
1311 anion-exchange chromatography with pulsed amperometric detection, *Atmos.*
1312 *Environ.*, 2006,40, S299-S311, <https://doi.org/10.1016/j.atmosenv.2005.12.069>,
1313 2006.

1314 Engling, G., Lee, J. J., Tsai, Y. W., Lung, S. H., C., C., Chou, C. K., and Chan, C.:
1315 Size-Resolved Anhydrosugar Composition in Smoke Aerosol from Controlled
1316 Field Burning of Rice Straw, *Aerosol Sci. Technol.*, 43, 662-672,
1317 <https://doi.org/10.1080/02786820902825113>, 2009.

1318 Fang, W., Andersson, A., Zheng, M., Lee, M., Holmstrand, H., Kim, S. W., Du, K.,
1319 and Örjan, G.: Divergent Evolution of Carbonaceous Aerosols during Dispersal
1320 of East Asian Haze, *Sci. Rep.*, 7, 10422,
1321 <https://doi.org/10.1038/s41598-017-10766-4>, 2017.

1322 Feng, Y. L., Chen, Y. J., Guo, H., Zhi, G. R., Xiong, S. C., Li, J., Sheng, G. Y., and Fu,
1323 J. M.: Characteristics of organic and elemental carbon in PM2.5 samples in
1324 Shanghai, China, *Atmos. Res.*, 92, 434-442,
1325 <https://doi.org/10.1016/j.atmosres.2009.01.003>, 2009.

1326 Fu, P. Q., Kawamura, K., Chen, J., Li, J., Sun, Y. L., Liu, Y., Tachibana, E., Aggarwal,
1327 S. G., Okuzawa, K., Tanimoto, H., Kanaya, Y., and Wang, Z. F.: Diurnal
1328 variations of organic molecular tracers and stable carbon isotopic composition in
1329 atmospheric aerosols over Mt. Tai in the North China Plain: an influence of
1330 biomass burning, *Atmos. Chem. Phys.*, 12, 8359-8375,
1331 <https://doi.org/10.5194/acp-12-8359-2012>, 2012.

1332 Gao, J. J., Wang, K., Wang, Y., Liu, S. H., Zhu, C. Y., Hao, J. M., Liu, H. J., Hua, S.
1333 B., and Tian, H. Z.: Temporal-spatial characteristics and source apportionment of
1334 PM2.5 as well as its associated chemical species in the Beijing-Tianjin-Hebei
1335 region of China, *Environ. Pollut.*, 233, 714-724,
1336 <https://doi.org/10.1016/j.envpol.2017.10.123>, 2018.

1337 Gelencsér, A., May, B., Simpson, D., Sánchez-Ochoa, A., Kasper-Giebl, A., Puxbaum,
1338 H., Caseiro, A., Pio, C., and Legrand, M.: Source apportionment of PM2.5

1339 organic aerosol over Europe: Primary/secondary, natural/anthropogenic, and
1340 fossil/biogenic origin, *J. Geophys. Res.: Atmos.*, 112,
1341 <https://doi.org/10.1029/2006jd008094>, 2007.

1342 Genberg, J., Hyder, M., Stenström, K., Bergström, R., Simpson, D., Fors, E. O.,
1343 Jönsson, J. A., and Swietlicki, E.: Source apportionment of carbonaceous aerosol
1344 in southern Sweden, *Atmos. Chem. Phys.*, 11, 13575-13616,
1345 <https://doi.org/10.5194/acp-11-11387-2011>, 2011.

1346 Guo, J. D., Ge, Y. S., Hao, L. J., Tan, J. W., Li, J. Q., and Feng, X. Y.: On-road
1347 measurement of regulated pollutants from diesel and CNG buses with urea
1348 selective catalytic reduction systems, *Atmos. Environ.*,
1349 <https://doi.org/10.1016/j.atmosenv.2014.07.032>, 2014.

1350 Hammer, S., and Levin, I.: Monthly mean atmospheric D14CO2 at Jungfraujoch and
1351 Schauinsland from 1986 to 2016, *Tellus B*, 65, 20092,
1352 <https://doi.org/10.11588/data/10100>, 2017.

1353 Han, R., Wang, S. X., Shen, W. H., Wang, J. D., Wu, K., Ren, Z. H., and Feng, M. N.:
1354 Spatial and temporal variation of haze in China from 1961 to 2012, *J. Environ.*
1355 *Sci.*, 46, 1001-0742, <https://doi.org/10.1016/j.jes.2015.12.033>, 2016a.

1356 Han, Y. M., Chen, L. W., Huang, R. J., Chow, J. C., Watson, J. G., Ni, H. Y., Liu, S. X.,
1357 Fung, K. K., Shen, Z. X., Wei, C., Wang, Q. Y., J. Tian, Zhao, Z. Z., Prévôt, A. S.
1358 H., and Cao, J. J.: Carbonaceous aerosols in megacity Xi'an, China: Implications
1359 of thermal/optical protocols comparison, *Atmos. Environ.*,
1360 <https://doi.org/10.1016/j.atmosenv.2016.02.023>, 2016b.

1361 Heal, M. R.: The application of carbon-14 analyses to the source apportionment of
1362 atmospheric carbonaceous particulate matter: a review, *Anal. Bioanal. Chem.*,
1363 406, 81–98, <https://doi.org/10.1007/s00216-013-7404-1>, 2014.

1364 Ho, K. F., Lee, S. C., Cao, J. J., Li, Y. S., Chow, J. C., Watson, J. G., and Fung, K.:
1365 Variability of organic and elemental carbon, water soluble organic carbon, and
1366 isotopes in Hong Kong, *Atmos. Chem. Phys.*, 6, 4569–4576,
1367 <https://doi.org/10.5194/acp-6-4569-2006>, 2006.

1368 Hoffmann, D., Tilgner, A., Iinuma, Y., and Herrmann, H.: Atmospheric stability of
1369 levoglucosan: a detailed laboratory and modeling study, *Environ. Sci. Technol.*,
1370 44, 694–699, <https://doi.org/10.1021/es902476f>, 2010.

1371 Hoyle, C. R., Boy, M., Donahue, N. M., Fry, J. L., Glasius, M., Guenther, A., Hallar,
1372 A. G., Hartz, K. H., Petters, M., Petřá T., Rosenoern, T., and Sullivan, A. P.: A
1373 review of the anthropogenic influence on biogenic secondary organic aerosol,
1374 *Atmos. Chem. Phys.*, 11, <https://doi.org/10.5194/acp-11-321-2011>, 2011.

1375 Hua, Q., and Barbetti, M.: Review of Tropospheric Bomb ¹⁴C Data for Carbon Cycle
1376 Modeling and Age Calibration Purposes, *Radiocarbon*, 46,
1377 <https://doi.org/10.1017/S0033822200033142>, 2004.

1378 Huang, J., Kang, S. C., Shen, C. D., Cong, Z. Y., Liu, K. X., Wang, W., and Liu, L. C.:
1379 Seasonal variations and sources of ambient fossil and biogenic-derived
1380 carbonaceous aerosols based on ¹⁴C measurements in Lhasa, Tibet, *Atmos. Res.*,
1381 96, 553–559, <https://doi.org/10.1016/j.atmosres.2010.01.003>, 2010.

1382 Huang, L., Brook, J. R., Zhang, W., Li, S. M., Graham, L., Ernst, D., Chivulescu, A.,
1383 and Lu, G.: Stable isotope measurements of carbon fractions (OC/EC) in
1384 airborne particulate: A new dimension for source characterization and
1385 apportionment, *Atmos. Environ.*, 40, 2690–2705,
1386 <https://doi.org/10.1016/j.atmosenv.2005.11.062>, 2006.

1387 Huang, R. J., Zhang, Y. L., Bozzetti, C., Ho, K. F., Cao, J. J., Han, Y. M., Dällenbach,
1388 K. R., Slowik, J. G., Platt, S. M., Canonaco, F., Zotter, P., Wolf, R., Pieber, S. M.,

1389 Bruns, E. A., Crippa, M., Ciarelli, G., Piazzalunga, A., Schwikowski, M.,
1390 Abbaszade, G., Schnelle-Kreis, J., Zimmermann, R., An, Z., Szidat, S.,
1391 Baltensperger, U., Haddad, I. E., and Prévôt, A.: High secondary aerosol
1392 contribution to particulate pollution during haze events in China, *Nature*, 514,
1393 218-222, <https://doi.org/10.1038/nature13774>, 2014.

1394 Jacobson, M. C., Hansson, H.-C., Noone, K. J., and Charlson, R. J.: Organic
1395 atmospheric aerosols: Review and state of the science, *Rev. Geophys.*, 38,
1396 267-294, <https://doi.org/10.1029/1998RG000045>, 2000.

1397 Jacobson, M. Z.: Strong radiative heating due to the mixing state of black carbon in
1398 atmospheric aerosols, *Nature*, <https://doi.org/10.1038/35055518>, 2001.

1399 Ji, D. S., Yan, Y. C., Wang, Z. S., He, J., Liu, B. X., Sun, Y., Gao, M., Li, Y., Cao, W.,
1400 Cui, Y., Hu, B., Xin, J. Y., Wang, L. L., Liu, Z. R., Tang, G. Q., and Wang, Y. S.:
1401 Two-year continuous measurements of carbonaceous aerosols in urban Beijing,
1402 China: Temporal variations, characteristics and source analyses, *Chemosphere*,
1403 200, 191-200, <https://doi.org/10.1016/j.chemosphere.2018.02.067>, 2018.

1404 Jimenez, J. L., Canagaratna, M. R., Donahue, N. M., Prevot, A. S. H., Zhang, Q.,
1405 Kroll, J. H., DeCarlo, P. F., Allan, J. D., Coe, H., Ng, N. L., Aiken, A. C.,
1406 Docherty, K. S., Ulbrich, I. M., Grieshop, A. P., Robinson, A. L., Duplissy, J.,
1407 Smith, J. D., Wilson, K. R., Lanz, V. A., Hueglin, C., Sun, Y. L., Tian, J.,
1408 Laaksonen, A., Raatikainen, T., Rautiainen, J., Vaattovaara, P., Ehn, M., Kulmala,
1409 M., Tomlinson, J. M., Collins, D. R., Cubison, M. J., Dunlea, J., Huffman, J. A.,
1410 Onasch, T. B., Alfarra, M. R., Williams, P. I., Bower, K., Kondo, Y., Schneider, J.,
1411 Drewnick, F., Borrmann, S., Weimer, S., Demerjian, K., Salcedo, D., Cottrell, L.,
1412 Griffin, R., Takami, A., Miyoshi, T., Hatakeyama, S., Shimojo, A., Sun, J. Y.,
1413 Zhang, Y. M., Dzepina, K., Kimmel, J. R., Sueper, D., Jayne, J. T., Herndon, S.

1414 C., Trimborn, A. M., Williams, L. R., Wood, E. C., Middlebrook, A. M., Kolb, C.
1415 E., Baltensperger, U., and Worsnop, D. R.: Evolution of Organic Aerosols in the
1416 Atmosphere, *Science*, 326, 1525-1529, <https://doi.org/10.1126/science.1180353>,
1417 2009.

1418 Jull, A. J. T.: Radiocarbon dating| AMS method, in: *Encyclopedia of Quaternary*
1419 *science* 2911-2918, 2007.

1420 Kawashima, H., and Haneishi, Y.: Effects of combustion emissions from the Eurasian
1421 continent in winter on seasonal $\delta^{13}\text{C}$ of elemental carbon in aerosols in Japan,
1422 *Atmos. Environ.*, 46, 568-579, <https://doi.org/10.1016/j.atmosenv.2011.05.015>,
1423 2012.

1424 Kiehl, J.: Twentieth century climate model response and climate sensitivity, *Geophys.*
1425 *Res. Lett.*, 34, 22710, <https://doi.org/10.1029/2007GL031383>, 2007.

1426 Kirillova, E. N., Andersson, A., Sheesley, R. J., Kruså M., Praveen, P. S., Budhavant,
1427 K., Safai, P. D., Rao, P., and Gustafsson, Ö.: ^{13}C - And ^{14}C -based study of
1428 sources and atmospheric processing of water-soluble organic carbon (WSOC) in
1429 South Asian aerosols, *Journal of Geophysical Research Atmospheres*, 118,
1430 614-626, <https://doi.org/10.1002/jgrd.50130>, 2013.

1431 Kumagai, K., Iijima, A., Shimoda, M., Saitoh, Y., Kozawa, K., Hagino, H., and
1432 Sakamoto, K.: Determination of Dicarboxylic Acids and Levoglucosan in Fine
1433 Particles in the Kanto Plain, Japan, for Source Apportionment of Organic
1434 Aerosols, *Aerosol Air Qual. Res.*, 10, 282-291,
1435 <https://doi.org/10.4209/aaqr.2009.11.0075>, 2010.

1436 Levin, I., Kromer, B., Schmidt, M., and Sartorius, H.: A novel approach for
1437 independent budgeting of fossil fuel CO_2 over Europe by $^{14}\text{CO}_2$ observations,
1438 *Geophys. Res. Lett.*, 30, <https://doi.org/10.1029/2003GL018477>, 2003.

1439 Levin, I., Naegler, T., Kromer, B., Diehl, M., Francey, R., Gomez Pelaez, A., Steele, P.,
1440 Wagenbach, D., Weller, R., and Worthy, D.: Observations and modelling of the
1441 global distribution and long-term trend of atmospheric $^{14}\text{CO}_2$, *Tellus B*, 62,
1442 26-46, <https://doi.org/10.1111/j.1600-0889.2009.00446.x>, 2010.

1443 Lewis, C. W., Klouda, G. A., and Ellenson, W. D.: Radiocarbon measurement of the
1444 biogenic contribution to summertime PM-2.5 ambient aerosol in Nashville, TN,
1445 *Atmos. Environ.*, 38, 6053-6061, <https://doi.org/10.1016/j.atmosenv.2004.06.011>,
1446 2004.

1447 Li, C. L., Bosch, C., Kang, S. C., Andersson, A., Chen, P. F., Zhang, Q. G., Cong, Z.
1448 Y., Chen, B., Qin, D. H., and Gustafsson, Ö.: Sources of black carbon to the
1449 Himalayan-Tibetan Plateau glaciers, *Nat. Commun.*, 7, 12574,
1450 <https://doi.org/10.1038/ncomms12574>, 2016.

1451 Li, H. M., Yang, Y., Wang, H. L., Li, B. J., Wang, P. Y., Li, J. D., and Liao, H.:
1452 Constructing a spatiotemporally coherent long-term PM_{2.5} concentration dataset
1453 over China during 1980–2019 using a machine learning approach, *Sci. Total*
1454 *Environ.*, 765, 0048-9697, <https://doi.org/10.1016/j.scitotenv.2020.144263>,
1455 2021a.

1456 Li, X. R., Wang, Y. S., Guo, X. Q., and Wang, Y. F.: Seasonal variation and source
1457 apportionment of organic and inorganic compounds in PM_{2.5} and PM₁₀
1458 particulates in Beijing, China, *J. Environ. Sci.*, 25, 741-750,
1459 [https://doi.org/10.1016/S1001-0742\(12\)60121-1](https://doi.org/10.1016/S1001-0742(12)60121-1), 2013.

1460 Li, Y. M., Fu, T.-M., Yu, J. Z., Feng, X., Zhang, L. J., Chen, J., Boreddy, S. K. R.,
1461 Kawamura, K., Fu, P., Yang, X., Zhu, L., and Zeng, Z. Z.: Impacts of chemical
1462 degradation on the global budget of atmospheric levoglucosan and its use as a
1463 biomass burning tracer, *Environ. Sci. Technol.*, 55, 5525-5536,

1464 <https://doi.org/10.1021/acs.est.0c07313>, 2021b.

1465 Liao, C. P., Wu, C. Z., Yan, y. J., and Huang, H. T.: Chemical elemental characteristics
1466 of biomass fuels in China, *Biomass Bioenergy*, 27, 119-130,
1467 <https://doi.org/10.1016/j.biombioe.2004.01.002>, 2004.

1468 Lim, S., Yang, X., Lee, M., Li, G., Jeon, K., Lim, S. H., YangYang, X., Lee, M. H., Li,
1469 G., Gao, Y. G., Shang, X. N., Zhang, K., I.Czimeczik, C., Xu, X. M., Min-SukBae,
1470 Moon, K.-J., and Jeon, K.: Fossil-driven secondary inorganic PM_{2.5}
1471 enhancement in the North China Plain: Evidence from carbon and nitrogen
1472 isotopes, *Environ. Pollut.*, 266, 115163,
1473 <https://doi.org/10.1016/j.envpol.2020.115163>, 2020.

1474 Liu, D., Li, J., Zhang, Y. L., Xu, Y., Liu, X., Ping, D., Shen, C. D., Chen, Y. J., Tian,
1475 C., and Zhang, G.: The Use of Levoglucosan and Radiocarbon for Source
1476 Apportionment of PM_{2.5} Carbonaceous Aerosols at a Background Site in East
1477 China, *Environ. Sci. Technol.*, 47, <https://doi.org/10.1021/es401250k>, 2013.

1478 Liu, J., Mo, Y., Li, J., Liu, D., Shen, C., Ding, P., Jiang, H., Cheng, Z., Zhang, X., and
1479 Tian, C.: Radiocarbon-derived source apportionment of fine carbonaceous
1480 aerosols before, during, and after the 2014 Asia-Pacific Economic Cooperation
1481 (APEC) summit in Beijing, China, *J. Geophys. Res.: Atmos.*, 121, 4177-4187,
1482 <https://doi.org/10.5194/acp-16-2985-2016>, 2016a.

1483 Liu, J. W., Li, J., Liu, D., Ding, P., Shen, C. D., Mo, Y. Z., Wang, X. M., Luo, C. L.,
1484 Cheng, Z. N., Szidat, S., Zhang, Y. L., Chen, Y. J., and Zhang, G.: Source
1485 apportionment and dynamic changes of carbonaceous aerosols during the haze
1486 bloom-decay process in China based on radiocarbon and organic molecular tracer,
1487 *Atmos. Chem. Phys.*, 16, 2985–2996, <https://doi.org/10.5194/acp-16-2985-2016>,
1488 2016b.

1489 Liu, Y., Shao, M., Fu, L. L., Lu, S. H., Zeng, L. M., and Tang, D. G.: Source profiles
1490 of volatile organic compounds (VOCs) measured in China: Part I, *Atmos.*
1491 *Environ.*, 42, 6247-6260, <https://doi.org/10.1016/j.atmosenv.2008.01.070>, 2008.

1492 Liu, Z. R., Hu, B., Liu, Q., Sun, Y., and Wang, Y. S.: Source apportionment of urban
1493 fine particle number concentration during summertime in Beijing, *Atmos.*
1494 *Environ.*, 96, 359-369, <https://doi.org/10.1016/j.atmosenv.2014.06.055>, 2014.

1495 Locker, H. B.: The use of levoglucosan to assess the environmental impact of
1496 residential wood-burning on air quality, Hanover, NH (US); Dartmouth College,
1497 1988.

1498 Lopez-Veneroni, D.: The stable carbon isotope composition of PM_{2.5} and PM₁₀ in
1499 Mexico City Metropolitan Area air, *Atmos. Environ.*, 43, 4491-4502,
1500 <https://doi.org/10.1016/j.atmosenv.2009.06.036>, 2009.

1501 Lu, L., Tang, Y., Xie, J. S., and Yuan, Y. L.: The role of marginal agricultural
1502 land-based mulberry planting in biomass energy production, *Renewable Energy*,
1503 34, 1789-1794, <https://doi.org/10.1016/j.renene.2008.12.017>, 2009.

1504 Martinelli, L. A., Camargo, P. B., Lara, L., Victoria, R. L., and Artaxo, P.: Stable
1505 carbon and nitrogen isotopic composition of bulk aerosol particles in a C4 plant
1506 landscape of southeast Brazil, *Atmos. Environ.*, 36, 2427-2432,
1507 [https://doi.org/10.1016/S1352-2310\(01\)00454-X](https://doi.org/10.1016/S1352-2310(01)00454-X), 2002.

1508 MEE: (Ministry of Ecology and Environment of the People's Republic of China):
1509 Technical Regulation on Ambient Air Quality Index, China Environmental
1510 Science Press (HJ 633-2012),
1511 [http://www.mee.gov.cn/ywgz/fgbz/bz/bzwb/jcffbz/201203/t20120302_224166.sh](http://www.mee.gov.cn/ywgz/fgbz/bz/bzwb/jcffbz/201203/t20120302_224166.shtml)
1512 [tml](#), 2012 (last access: 28 March 2022).

1513 MEE: (Ministry of Ecology and Environment of the People's Republic of China):

1514 Bulletin of Ecology and Environment of the People's Republic of China 2013,
1515 [http://www.mee.gov.cn/hjzl/sthjzk/zghjzkgb/201605/P020160526564730573906.](http://www.mee.gov.cn/hjzl/sthjzk/zghjzkgb/201605/P020160526564730573906.pdf)
1516 [pdf](#), 2014 (last access: 28 March 2022).

1517 MEE: (Ministry of Ecology and Environment of the People's Republic of China):
1518 Bulletin of Ecology and Environment of the People's Republic of China 2018,
1519 [http://www.mee.gov.cn/hjzl/sthjzk/zghjzkgb/201905/P020190619587632630618.](http://www.mee.gov.cn/hjzl/sthjzk/zghjzkgb/201905/P020190619587632630618.pdf)
1520 [pdf](#), 2019 (last access: 28 March 2022).

1521 MEE: (Ministry of Ecology and Environment of the People's Republic of China):
1522 Bulletin of Ecology and Environment of the People's Republic of China 2019,
1523 [http://www.mee.gov.cn/hjzl/sthjzk/zghjzkgb/202006/P020200602509464172096.](http://www.mee.gov.cn/hjzl/sthjzk/zghjzkgb/202006/P020200602509464172096.pdf)
1524 [pdf](#), 2020 (last access: 28 March 2022).

1525 MEE: (Ministry of Ecology and Environment of the People's Republic of China):
1526 Bulletin of Ecology and Environment of the People's Republic of China 2020,
1527 [http://www.mee.gov.cn/hjzl/sthjzk/zghjzkgb/202105/P020210526572756184785.](http://www.mee.gov.cn/hjzl/sthjzk/zghjzkgb/202105/P020210526572756184785.pdf)
1528 [pdf](#), 2021 (last access: 28 March 2022).

1529 Mook, W. G., and Plicht, J. V. D.: Reporting 14C Activities and Concentrations,
1530 Radiocarbon, 41, 227-239, <https://doi.org/10.1017/S0033822200057106>, 1999.

1531 Moura, J. M. S., Martens, C. S., Moreira, M. Z., Lima, R. L., Sampaio, I. C. G.,
1532 Mendlovitz, H. P., and Menton, M. C.: Spatial and seasonal variations in the
1533 stable carbon isotopic composition of methane in stream sediments of eastern
1534 Amazonia, Tellus B, 60, 21-31,
1535 <https://doi.org/10.1111/j.1600-0889.2007.00322.x>, 2008.

1536 NBS: (National bureau of statistics): China Statistical Yearbook-2019, China Statistics
1537 press <http://www.stats.gov.cn/tjsj/ndsj/2019/indexch.htm>, 2020 (last access: 28
1538 March 2022).

1539 NBS: (National bureau of statistics): China Statistical Yearbook-2020, China Statistics
1540 press, <http://www.stats.gov.cn/tjsj/ndsj/2020/indexch.htm>, 2021 (last access: 28
1541 March 2022).

1542 Ni, H. Y., Huang, R. J., Cao, J. J., Liu, W. G., Zhang, T., Wang, M., Meijer, H. A., and
1543 Dusek, U.: Source apportionment of carbonaceous aerosols in Xi'an, China:
1544 insights from a full year of measurements of radiocarbon and the stable isotope
1545 C-13, *Atmos. Chem. Phys.*, <https://doi.org/10.5194/acp-18-16363-2018>, 2018.

1546 Ni, H. Y., Huang, R. J., Cosijn, M. M., Yang, L., and Dusek, U.: Measurement report:
1547 dual-carbon isotopic characterization of carbonaceous aerosol reveals different
1548 primary and secondary sources in Beijing and Xi'an during severe haze events,
1549 *Atmos. Chem. Phys.*, 20, 16041-16053,
1550 <https://doi.org/10.5194/acp-20-16041-2020>, 2020.

1551 Niu, Z. C., Wang, S., Chen, J. S., Zhang, F. W., Chen, X. Q., He, C., Lin, L. F., Yin, L.
1552 Q., and Xu, L. L.: Source contributions to carbonaceous species in PM_{2.5} and
1553 their uncertainty analysis at typical urban, peri-urban and background sites in
1554 southeast China, *Environ. Pollut.*, 181, 107-114,
1555 <https://doi.org/10.1016/j.envpol.2013.06.006>, 2013.

1556 Niu, Z. C., Zhou, W. J., Cheng, P., Wu, S. G., Lu, X. F., Xiong, X. H., Du, H., and Fu,
1557 Y. C.: Observations of Atmospheric $\Delta^{14}\text{CO}_2$ at the Global and Regional
1558 Background Sites in China: Implication for Fossil Fuel CO_2 Inputs, *Environ.*
1559 *Sci. Technol.*, 50, 12122-12128, <https://doi.org/10.1021/acs.est.6b02814>, 2016.

1560 Niu, Z. C., Feng, X., Zhou, W. J., Wang, P., Liu, Y., Lu, X. F., Du, H., Fu, Y. C., Li, M.,
1561 Mei, R. C., Li, Q., and Cai, Q. F.: Tree-ring $\Delta^{14}\text{C}$ time series from 1948 to
1562 2018 at a regional background site, China: Influences of atmospheric nuclear
1563 weapons tests and fossil fuel emissions, *Atmos. Environ.*, 246,

1564 <https://doi.org/10.1016/j.atmosenv.2020.118156>, 2021.

1565 Novakov, T., Menon, S., Kirchstetter, T. W., Koch, D., and Hansen, J. E.: Aerosol
1566 organic carbon to black carbon ratios: Analysis of published data and
1567 implications for climate forcing, *Journal of Geophysical Research Atmospheres*,
1568 110, <https://doi.org/10.1029/2005JD005977>, 2005.

1569 Oros, D. R., and Simoneit, B. R. T.: Identification and emission factors of molecular
1570 tracers in organic aerosols from biomass burning Part 2. Deciduous trees, *Appl.*
1571 *Geochem.*, 16, 1545-1565, [https://doi.org/10.1016/s0883-2927\(01\)00022-1](https://doi.org/10.1016/s0883-2927(01)00022-1),
1572 2001a.

1573 Oros, D. R., and Simoneit, B. R. T.: Identification and emission factors of molecular
1574 tracers in organic aerosols from biomass burning Part 1. Temperate climate
1575 conifers, *Appl. Geochem.*, 16, 1513-1544,
1576 [https://doi.org/10.1016/s0883-2927\(01\)00021-x](https://doi.org/10.1016/s0883-2927(01)00021-x), 2001b.

1577 PGHP: (The People's Government of Hebei Province): Hebei Economic
1578 Yearbook-2020, China Statistics press,
1579 <http://tjj.hebei.gov.cn/hetj/tjnj/2020/indexch.htm>, 2021 (last access: 28 March
1580 2022).

1581 Popovicheva, O. B., Kozlov, V. S., Engling, G., Diapouli, E., Persiantseva, N. M.,
1582 Timofeev, M. A., Fan, T.-S., Saraga, D., and Eleftheriadis, K.: Small-scale study
1583 of siberian biomass burning: i. smoke microstructure, *Aerosol Air Qual. Res.*, 15,
1584 117-128, <https://doi.org/10.4209/aaqr.2014.09.0206>, 2014.

1585 Pugliese, S. C., Murphy, J. G., Vogel, F., and Worthy, D.: Characterization of the d13C
1586 signatures of anthropogenic CO2 emissions in the Greater Toronto Area, Canada,
1587 *Appl. Geochem.*, 83, 171-1800,
1588 <https://doi.org/10.1016/j.apgeochem.2016.11.003>, 2017.

1589 Puxbaum, H., Caseiro, A., Sánchez-Ochoa, A., Kasper-Giebl, A., Claeys, M.,
1590 Gelencsér, A., Legrand, M., Preunkert, S., and Pio, C.: Levoglucosan levels at
1591 background sites in Europe for assessing the impact of biomass combustion on
1592 the European aerosol background, *J. Geophys. Res.*, 112, D23S05,
1593 <https://doi.org/10.1029/2006jd008114>, 2007.

1594 Rajput, P., Sarin, M. M., Rengarajan, R., and Singh, D.: Atmospheric polycyclic
1595 aromatic hydrocarbons (pahs) from post-harvest biomass burning emissions in
1596 the indo-gangetic plain: isomer ratios and temporal trends, *Atmospheric*
1597 *Environment*, 45, 6732-6740, <https://doi.org/10.1016/j.atmosenv.2011.08.018>,
1598 2011.

1599 SAPBS: (Shaanxi Provincial Bureau of Statistics): Shaanxi Statistical Yearbook-2020,
1600 China Statistics press, <http://tjj.shaanxi.gov.cn/upload/n2020/indexch.htm>, 2020
1601 (last access: 28 March 2022).

1602 Seinfeld, J. H., and Pandis, S. N.: *Atmospheric Chemistry and Physics: From Air*
1603 *Pollution to Climate Change*, Environ.: Sci. Policy Sustainable Dev., 1998.

1604 Shang, J., Khuzestani, R. B., Tian, J., Schauer, J. J., Hua, J., Zhang, Y., Cai, T., Fang,
1605 D., An, J., and Zhang, Y.: Chemical characterization and source apportionment of
1606 PM_{2.5} personal exposure of two cohorts living in urban and suburban Beijing,
1607 *Environ. Pollut.*, <https://doi.org/10.1016/j.envpol.2018.11.076>, 2019.

1608 Shao, M., Li, J., and Tang, X.: The application of accelerator mass spectrometry
1609 (AMS) in the study of source identification of aerosols (in Chinese). *Acta*
1610 *Scientiae Circumstantiae* 16 (2), 130–141, 1996.

1611 Shen, G. F., Wang, W., Yang, Y. F., Zhu, C., Min, Y. J., Xue, M., Ding, J. N., Li, W.,
1612 Wang, B., Shen, H. Z., Wang, R., Wang, X. L., and Tao, S.: Emission factors and
1613 particulate matter size distribution of polycyclic aromatic hydrocarbons from

1614 residential coal combustions in rural Northern China, *Atmos. Environ.*, 44,
1615 5237-5243, <https://doi.org/10.1016/j.atmosenv.2010.08.042>, 2010.

1616 Shen, Z. X., Cao, J. J., Liu, S. X., Zhu, C. S., Wang, X., Zhang, T., Xu, H. M., and Hu,
1617 T. F.: Chemical Composition of PM₁₀ and PM_{2.5} Collected at Ground Level and
1618 100 Meters during a Strong Winter-Time Pollution Episode in Xi'an, China, *J.*
1619 *Air Waste Manage. Assoc.*, <https://doi.org/10.1080/10473289.2011.608619>,
1620 2011.

1621 Simoneit, B. R. T., Schauer, J. J., Nolte, C. G., Oros, D. R., Elias, V. O., Fraser, M. P.,
1622 Rogge, W. F., and Cass, G. R.: Levoglucosan, a tracer for cellulose in biomass
1623 burning and atmospheric particles, *Atmos. Environ.*, 33, 173-182,
1624 [https://doi.org/10.1016/S1352-2310\(98\)00145-9](https://doi.org/10.1016/S1352-2310(98)00145-9), 1999.

1625 Simpson, D., Yttri, K. E., Klimont, Z., Kupiainen, K., Caseiro, A., Gelencsér, A., Pio,
1626 C., Puxbaum, H., and Legrand, M.: Modeling carbonaceous aerosol over Europe:
1627 Analysis of the CARBOSOL and EMEP EC/OC campaigns, *Journal of*
1628 *Geophysical Research Atmospheres*, 112, -,
1629 <https://doi.org/10.1029/2006JD008158>, 2007.

1630 Slota, P. J., Jull, A. J. T., Linick, T. W., and Toolin, L. J.: Preparation of Small Samples
1631 for ¹⁴C Accelerator Targets by Catalytic Reduction of CO, *Radiocarbon*, 29,
1632 303-306, <https://doi.org/10.1017/S0033822200056988>, 1987.

1633 Smith, B. N., and Epstein, S.: Two Categories of ¹³C/¹²C Ratios for Higher Plants,
1634 *Plant Physiol.*, 47, 380-384, <https://doi.org/10.1029/2006JD008158>, 1971.

1635 Song, Y., Zhang, Y. H., Xie, S. D., Zeng, L. M., Zheng, M., Salmon, L., Shao, M., and
1636 Slanina, S.: Source apportionment of PM_{2.5} in Beijing by positive matrix
1637 factorization, *Atmos. Environ.*, 40, 1526-1537,
1638 <https://doi.org/10.1016/j.atmosenv.2005.10.039>, 2006.

1639 SPBS: (Shanxi Provincial Bureau of Statistics): Shanxi Statistical Yearbook-2019,
1640 China Statistics press,
1641 <http://tjj.shaanxi.gov.cn/upload/2020/pro/3sxtjni/zk/indexch.htm>, 2020 (last
1642 access: 28 March 2022).

1643 Streets, D. G., Bond, T. C., Carmichael, G. R., Fernandes, S. D., Fu, Q., He, D.,
1644 Klimont, Z., Nelson, S. M., Tsai, N. Y., Wang, M. Q., Woo, J. H., and Yarber, K.
1645 F.: An inventory of gaseous and primary aerosol emissions in Asia in the year
1646 2000, *J. Geophys. Res.: Atmos.*, 108, <https://doi.org/10.1029/2002JD003093>,
1647 2003a.

1648 Streets, D. G., Yarber, K. F., Woo, J.-H., and Carmichael, G. R.: Biomass burning in
1649 Asia: Annual and seasonal estimates and atmospheric emissions, *Global*
1650 *Biogeochem. Cycles*, 17, 1099, <https://doi.org/10.1029/2003GB002040>, 2003b.

1651 Stuiver, M., and Polach, H.: Discussion: Reporting of ¹⁴C data, *Radiocarbon*, 19,
1652 355-363, <https://doi.org/10.1017/S0033822200003672>, 1977.

1653 Sun, X. S., Hu, M., Guo, S., Liu, K. X., and Zhou, L. P.: ¹⁴C-Based source
1654 assessment of carbonaceous aerosols at a rural site, *Atmos. Environ.*, 50, 36-40,
1655 <https://doi.org/10.1016/j.atmosenv.2012.01.008>, 2012.

1656 Sun, Y. L., Zhuang, G. S., Tang, A. H., Wang, Y., and An, Z. S.: Chemical
1657 characteristics of PM_{2.5} and PM₁₀ in haze-fog episodes in Beijing, *Environ. Sci.*
1658 *Technol.*, 40, 3148-3155, <https://doi.org/10.1021/es051533g>, 2006.

1659 Szidat, S., Jenk, T. M., Gaeggeler, H. W., Synal, H. A., Hajdas, I., Bonani, G., and
1660 Saurer, M.: THEODORE, a two-step heating system for the EC/OC
1661 determination of radiocarbon (¹⁴C) in the environment, *Nucl. Instrum. Methods*
1662 *Phys. Res.*, 223, 829-836, <https://doi.org/10.1016/j.nimb.2004.04.153>, 2004.

1663 Szidat, S., Jenk, T. M., Synal, H., Kalberer, M., Wacker, L., Hajdas, I., Kasper-Giebl,

1664 A., and Baltensperger, U.: Contributions of fossil fuel, biomass burning, and
1665 biogenic emissions to carbonaceous aerosols in Zürich as traced by ^{14}C , Journal
1666 of Geophysical Research Atmospheres, 111, -,
1667 <http://doi.org/10.1029/2005JD006590>, 2006.

1668 Szidat, S., Ruff, M., Perron, N., Wacker, L., Synal, H. A., Hallquist, M., Shannigrahi,
1669 A. S., Yttri, K., Dye, C., and Simpson, D.: Fossil and non-fossil sources of
1670 organic carbon (OC) and elemental carbon (EC) in Göteborg, Sweden, Atmos.
1671 Chem. Phys., 9, 16255-16289, <https://doi.org/10.5194/acpd-8-16255-2008>, 2009.

1672 Tanarit, S., Alex, G., Detlev, H., Jana, M., and Christine, W.: Secondary Organic
1673 Aerosol from Sesquiterpene and Monoterpene Emissions in the United States,
1674 Environ. Sci. Technol., 42, 8784–8790, <https://doi.org/10.1021/es800817r>, 2008.

1675 Tian, S. L., Pan, Y. P., and Wang, Y. S.: Size-resolved source apportionment of
1676 particulate matter in urban Beijing during haze and non-haze episodes, Atmos.
1677 Chem. Phys., 16, 9405-9443, <https://doi.org/10.5194/acp-16-1-2016>, 2016.

1678 Turekian, V. C., Macko, S., Ballentine, D., Swap, R. J., and Garstang, M.: Causes of
1679 bulk carbon and nitrogen isotopic fractionations in the products of vegetation
1680 burns: laboratory studies, Chem. Geol., 152, 181-192,
1681 [https://doi.org/10.1016/S0009-2541\(98\)00105-3](https://doi.org/10.1016/S0009-2541(98)00105-3), 1998.

1682 Turnbull, J. C., Lehman, S. J., Miller, J. B., Sparks, R. J., Southon, J. R., and Tans, P.
1683 P.: A new high precision ^{14}C time series for North American continental air, J.
1684 Geophys. Res., <http://doi.org/10.1029/2006jd008184>, 2007.

1685 Turpin, B. J., and Huntzicker, J. J.: Identification of secondary organic aerosol
1686 episodes and quantitation of primary and secondary organic aerosol
1687 concentrations during SCAQS, Atmos. Environ., 29, 3527-3544,
1688 [https://doi.org/10.1016/1352-2310\(94\)00276-Q](https://doi.org/10.1016/1352-2310(94)00276-Q), 1995.

1689 Vardag, S. N., Gerbig, C., Janssens-Maenhout, G., and Levin, I.: Estimation of
1690 continuous anthropogenic CO₂: model-based evaluation of CO₂, CO,
1691 D13C(CO₂) and D14C(CO₂) tracer methods, *Atmos. Chem. Phys.*, 15,
1692 12705–12729, <https://doi.org/10.5194/acp-15-12705-2015>, 2015.

1693 Vonwiller, M., Quintero, G. S., and Szidat, S.: Isolation and 14C analysis of
1694 humic-like substances (HULIS) from ambient aerosol samples,
1695 <https://doi.org/10.7892/boris.108864>, 2017.

1696 Wang, G., Cheng, S., Li, J., Lang, J., Wen, W., Yang, X., Tian, L., Wang, G., Cheng, S.
1697 Y., Li, J. B., Lang, J. L., Wen, W., Yang, X. W., and Tian, L.: Source
1698 apportionment and seasonal variation of PM_{2.5} carbonaceous aerosol in the
1699 Beijing-Tianjin-Hebei Region of China, *Environ. Monit. Assess.*, 187, 1-13,
1700 <https://doi.org/10.1007/s10661-015-4288-x>, 2015.

1701 Wang, H. L., Zhuang, Y. H., Wang, Y., Yuan, Y. L., and Zhuang, G. S.: Long-term
1702 monitoring and source apportionment of PM_{2.5}/PM₁₀ in Beijing, China, *J.*
1703 *Environ. Sci.*, 20, 1323-1327, [https://doi.org/10.1016/S1001-0742\(08\)62228-7](https://doi.org/10.1016/S1001-0742(08)62228-7),
1704 2008.

1705 Wang, X. F., Zhu, G. H., Wu, Y. G., and Shen, X. Y.: Chemical composition and size
1706 distribution of particles in the atmosphere in north part of Beijing city for winter
1707 and summer (In Chinese), *Chinese Journal of Atmospheric Sciences*, 14, 199-206,
1708 <https://doi.org/10.3878/j.issn.1006-9895.1990.02.09>, 1990.

1709 Wang, Z. Z., Bi, X. H., Sheng, G. Y., and Fu, J. M.: Characterization of organic
1710 compounds and molecular tracers from biomass burning smoke in South China I:
1711 Broad-leaf trees and shrubs, *Atmos. Environ.*, 43, 3096-3102,
1712 <https://doi.org/10.1016/j.atmosenv.2009.03.012>, 2009.

1713 Weber, R. J., Sullivan, A. P., Peltier, R. E., Russell, A., Yan, B., Zheng, M., Gouw, J.

1714 D., Warneke, C., Brock, C., and Holloway, J. S.: A study of secondary organic
1715 aerosol formation in the anthropogenic-influenced southeastern United States,
1716 Journal of Geophysical Research Atmospheres, 112, D13302,
1717 <https://doi.org/10.1029/2007jd008408>, 2007.

1718 Widory, D.: Combustibles, fuels and their combustion products: A view through
1719 carbon isotopes, Combust. Theor. Model., 10, 831-841,
1720 <https://doi.org/10.1080/13647830600720264>, 2006.

1721 Winiger, P., Andersson, A., Eckhardt, S., Stohl, A., Semiletov, I. P., Dudarev, O. V.,
1722 Charkin, A., Shakhova, N., Klimont, Z., and Heyes, C.: Siberian Arctic black
1723 carbon sources constrained by model and observation, Proc Natl Acad Sci U S A,
1724 114, E1054, <https://doi.org/10.1073/pnas.1613401114>, 2017.

1725 Wu, J., Kong, S. F., Zeng, X., Cheng, Y., Yan, Q., Zheng, H., Yan, Y. Y., Zheng, S. R.,
1726 Liu, D. T., Zhang, X. Y., Fu, P. Q., Wang, S. X., and Qi, S. H.: First
1727 High-Resolution Emission Inventory of Levoglucosan for Biomass Burning and
1728 Non-Biomass Burning Sources in China, Environ. Sci. Technol., 55, 1497-1507,
1729 <https://doi.org/10.1021/acs.est.0c06675>, 2021.

1730 XAMBS: (Xi'an Municipal Bureau Statistics): Xi'an Statistical Yearbook-2014,
1731 China Statistics press, <http://tjj.xa.gov.cn/tjnj/2014/tjnj/indexch.htm>, 2014 (last
1732 access: 28 March 2022).

1733 XAMBS: (Xi'an Municipal Bureau Statistics): Xi'an Statistical Yearbook-2020 China
1734 Statistics press, <http://tjj.xa.gov.cn/tjnj/2020/zk/indexch.htm>, 2021 (last access:
1735 28 March 2022).

1736 Yan, X. Y., Ohara, T., and Akimoto, H.: Bottom-up estimate of biomass burning in
1737 mainland china, Atmos. Environ., 40, 5262-5273,
1738 <https://doi.org/10.1016/j.atmosenv.2006.04.040>, 2006.

1739 Yan, X. Y., and Crookes, R. J.: Energy demand and emissions from road
1740 transportation vehicles in China, *Prog. Energy Combust. Sci.*, 36, 651-676,
1741 <https://doi.org/10.1016/j.pecs.2010.02.003>, 2010.

1742 Yang, F., He, K., Ye, B., Chen, X., Cha, L., Cadle, S. H., Chan, T., and Mulawa, P. A.:
1743 One-year record of organic and elemental carbon in fine particles in downtown
1744 Beijing and Shanghai, *Atmos. Chem. Phys.*, 5, 1449-1457,
1745 <https://doi.org/10.5194/acp-5-1449-2005>, 2005.

1746 Zhang, R., Jing, J., Tao, J., Hsu, S. C., Wang, G., Cao, J., Lee, C. S. L., Zhu, L., Chen,
1747 Z., and Zhao, Y.: Chemical characterization and source apportionment of PM_{2.5}
1748 in Beijing: seasonal perspective, *Atmos. Chem. Phys.*, 13, 7053-7074,
1749 <https://doi.org/10.5194/acp-14-175-2014>, 2014.

1750 Zhang, Y. L., Perron, N., Ciobanu, V. G., Zotter, P., and Szidat, S.: On the isolation of
1751 OC and EC and the optimal strategy of radiocarbon-based source apportionment
1752 of carbonaceous aerosols, *Soil Biol. Biochem.*, 12, 17657-17702,
1753 <https://doi.org/10.5194/acpd-12-17657-2012>, 2012.

1754 Zhang, Y. L., Huang, R. J., Haddad, I. E. I., Ho, K. F., Cao, J. J., Han, Y., Zotter, P.,
1755 Bozzetti, C., Daellenbach, K. R., Canonaco, F., Slowik, J. G., Salazar, G.,
1756 Schwikowski, M., Schnelle-Kreis, J., Abbaszade, G., Zimmermann, R.,
1757 Baltensperger, U., Prévôt, A. S. H., and Szidat, S.: Fossil vs. non-fossil sources
1758 of fine carbonaceous aerosols in four Chinese cities during the extreme winter
1759 haze episode of 2013, *Atmos. Chem. Phys.*, 15, 1299-1312,
1760 <https://doi.org/10.5194/acp-15-1299-2015>, 2015.

1761 Zhang, Y. L., Ren, H., Sun, Y. L., Cao, F., Chang, Y. H., Liu, S. D., Lee, X. H., Agrios,
1762 K., Kawamura, K., Liu, D., Ren, L. J., Du, W., Wang, Z. F., Prévôt, A. S. H.,
1763 Szidat, S., and Fu, P. Q.: High Contribution of Nonfossil Sources to

1764 Submicrometer Organic Aerosols in Beijing, China, *Environ. Sci. Technol.*, 51,
1765 7842, <https://doi.org/10.1021/acs.est.7b01517>, 2017a.

1766 Zhang, Y. X., Shao, M., Zhang, Y. H., Zeng, L. M., HE., L. Y., Zhu, B., Wei, Y. J., and
1767 Zhu, X. L.: Source profiles of particulate organic matters emitted from cereal
1768 straw burnings, *J. Environ. Sci.*, 19, 167-175,
1769 [https://doi.org/10.1016/S1001-0742\(07\)60027-8](https://doi.org/10.1016/S1001-0742(07)60027-8), 2007.

1770 Zhang, Z. S., Engling, G., Chan, C. Y., Yang, Y. H., Lin, M., Shi, S., He, J., Li, Y. D.,
1771 and Wang, X. M.: Determination of isoprene-derived secondary organic aerosol
1772 tracers (2-methyltetrols) by HPAEC-PAD: Results from size-resolved aerosols in
1773 a tropical rainforest, *Atmos. Environ.*, 70, 468-476,
1774 <https://doi.org/10.1016/j.atmosenv.2013.01.020>, 2013.

1775 Zhang, Z. S., Gao, J., Zhang, L. M., Wang, H., Tao, J., Qiu, X. H., Chai, F. H., Li, Y.,
1776 and Wang, S. L.: Observations of biomass burning tracers in pm 2.5 at two
1777 megacities in north china during 2014 apec summit, *Atmos. Environ.*, 169, 54-65,
1778 <http://dx.doi.org/10.1016/j.atmosenv.2017.09.011>, 2017b.

1779 Zhao, P. S., Dong, F., Yang, Y. D., He, D., Zhao, X. J., Zhang, W. Z., Yao, Q., and Liu,
1780 H. Y.: Characteristics of carbonaceous aerosol in the region of Beijing, Tianjin,
1781 and Hebei, China, *Atmos. Environ.*, 71, 389-398,
1782 <https://doi.org/10.1016/j.atmosenv.2013.02.010>, 2013.

1783 Zhao, Z. Z., Cao, J. J., Zhang, T., XingShen, Z., Ni, H. Y., Tian, J., Wang, Q. Y., Liu, S.
1784 X., Zhou, J. M., Gu, J., and Shen, G. Z.: Stable carbon isotopes and levoglucosan
1785 for pm 2.5 elemental carbon source apportionments in the largest city of
1786 northwest china, *Atmos. Environ.*, 185, 253-261,
1787 <https://doi.org/10.1016/j.atmosenv.2018.05.008>, 2018.

1788 Zhi, G. R., Chen, Y. J., Feng, Y. L., Xiong, S. C., Jun, L. I., Zhang, G., Sheng, G. Y.,

1789 and Jiamo, F. U.: Emission characteristics of carbonaceous particles from various
1790 residential coal-stoves in China, *Environ. Sci. Technol.*, 42, 3310,
1791 <https://doi.org/10.1021/es702247q>, 2008.

1792 Zhou, W. J., Zhao, X. L., Feng, L. X., Lin, L., Kun, W. Z., Peng, C., Nian, Z. W., and
1793 Hai, H. C.: The 3MV multi-element AMS in Xi'an, China: Unique features and
1794 preliminary tests, *Radiocarbon*, 48, 285-293,
1795 <https://doi.org/10.1017/S0033822200066492>, 2006.

1796 Zhou, W. J., Lua, X. F., Wu, Z. K., Zhao, W. N., Huang, C. H., Lia, L. L., Chen, P.,
1797 and Xin, Z. H.: New results on Xi'an-AMS and sample preparation systems at
1798 Xi'an-AMS center, *Nucl. Instrum. Methods Phys. Res.*, 262, 135-142,
1799 <https://doi.org/10.1016/j.nimb.2007.04.221>, 2007.

1800 Zhou, W. J., Wu, S. G., Huo, W. W., Xiong, X. H., Cheng, P., Lu, X. F., and Niu, Z. C.:
1801 Tracing fossil fuel CO₂ using $\Delta^{14}\text{C}$ in Xi'an City, China, *Atmos. Environ.*, 94,
1802 538-545, <https://doi.org/10.1017/S0033822200066492>, 2014.

1803